CHAPTER

6

Radiographic Examinations and Imaging of Patients with Lesions Affecting the Nervous System

Edward K. Mark, Jr.
Ramon E. Figueroa
Alexis Norelle

The technological evolution which has occurred in neuroradiology over the past 20 years is without parallel in clinical medicine and is a major factor in the development of neuroradiology as a distinct discipline within radiology.

This rapid acceleration of imaging technology was spawned by the development of computer-assisted imaging techniques such as computerized tomography (CT), magnetic resonance imaging (MRI), and ultrasonography (US). These techniques employ powerful computers and complex computer programs to collect, analyze, and reconstruct enormous amounts of data into digitized images.

From a clinical perspective, computer-assisted imaging techniques have greatly enhanced diagnostic sensitivity and specificity, with minimal risks to the patient. They have practically replaced certain traditional imaging methods such as pneumoencephalography and significantly limited the indications for others such as arteriography, myelography, and radioisotope scanning.

In this chapter we will attempt to convey what we believe are the essentials of contemporary neuroradiology as it is practiced at our institution. Emphasis has been placed on the computer-assisted imaging techniques—CT, MRI, and US—since these comprise the mainstay of our diagnostic imaging. Arteriography, myelography, and ultrasonography have been reviewed disproportionately to their relative application in contemporary neuroradiology; however, we feel this was necessary to clearly convey their essentials. Other techniques, such as pneumoencephalography, radioisotope scanning, positron emission tomography (PET) scanning, and diskography have received quite summary discussion, which is indicative of their limited use at our institution. This should not be interpreted as a condemnation.

Applications of the various imaging modalities to intracranial pathology are presented first, followed by their application to spinal pathology. Neurosonology is presented separately from other imaging techniques, primarily to limit the confusion that can occur when describing the physical and technical principles involved in different imaging modalities. Throughout this discussion, we have included numerous illustrations to support the text. Most of these describe normal anatomy or its variations. We have deferred presentation of images describing pathology to their respective chapters elsewhere in this book.

The conclusion provides a modest list of suggested review texts that give a more in-depth treatment of specific aspects of neuroradiology.

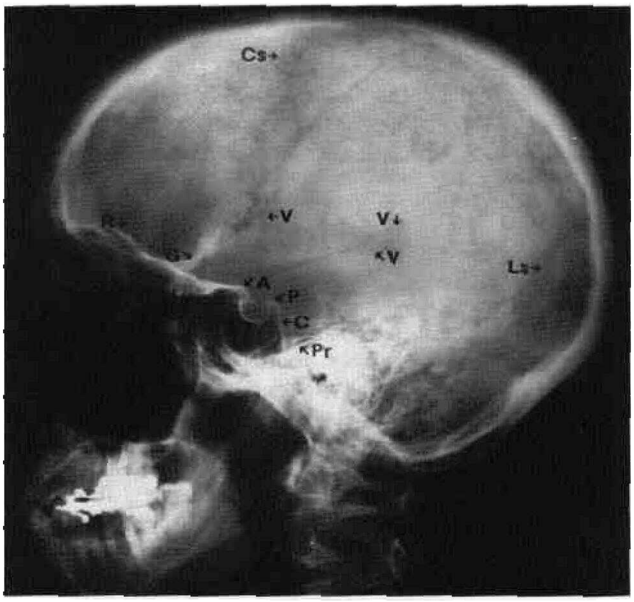

Figure 6-1 Lateral skull x-ray. A = antrerior clinoid; C = clivus; Cs = coronal suture; E = ethmoid air cells; F = floor of sella; Fs = frontal sinus; G = greater wing of the sphenoid; I = internal auditory canal; L = lesser wing of sphenoid; Ms = mastoid air cells; MX = maxillary sinus; N = nasal septum; P = posterior clinoid; Pr = petrous ridge; R = orbital roof; S = superior orbital fissure; Ss = sphenoid sinus; V = vascular grooves of meningeal vessels.

NEURORADIOLOGY OF THE HEAD

PLAIN SKULL RADIOGRAPHY

Traditionally, the radiographic investigation of suspected calvarial and intracranial lesions begins with a series of plain skull radiographs. A variety of projections £nd techniques for plain radiographs relate radiographic features to specific intracranial lesions as well as some systemic disease.[1] The major handicap of radiography of the skull arises from its inability to image intracranial lesions directly.

Direct imaging of intracranial lesions is best achieved by the use of computer-assisted imaging techniques, computerized tomography (CT), and magnetic resonance imaging (MRI). These provide the capability of obtaining high-resolution images and specific localization of intracranial lesions.

As a result, interest in plain skull radiographs has declined. Its principal application today is as a screening or adjunctive imaging technique in the evaluation of suspected calvarial lesions, such as bony metastatic disease, reactive or inflammatory bone disease, congenital skull deformities, and skull trauma. For the astute clinician, plain radiographs of the skull also reveal evidence of elevated intracranial pressure or space-occupying lesions, such as thinning of the cortical floor of the sella, displacement of the normally midline pineal gland, widening of the bony sutures in children, and enlargement of the vascular grooves. The most useful views for accomplishing these objectives include the following:

Lateral projection. Most useful for observation of patterns of intracranial and craniovertebral junction pathology (Fig. 6-1).
20° Anteroposterior (AP). Demonstrates the position of the calcified pineal gland.

In addition to the lateral and AP views, the standard skull series typically includes:

25° *Poster-oanterior (Cauldwell) view.* Useful in demonstration of fractures and lesions of the midfacial sinuses.
30° Anteroposterior (Townes) view. Useful in the demonstration of lesions involving the mastoid and petrous bones.
Submental vertex (Hirtz) view. May demonstrate abnormalities of the skull base foramina.

Additional applications of the skull x-ray to the neurosurgeon include the evaluation of ventricular or cisternal shunts for continuity and placement and the intraoperative localization of foreign bodies or outlining adjacent structures as is required in pituitary surgery. Figure 6-1 provides the essential anatomy of normal lateral skull x-rays.

INTRACRANIAL COMPUTERIZED TOMOGRAPHY

The introduction of CT in 1972 initiated a major evolution in the field of diagnostic neuroimaging with its ability to

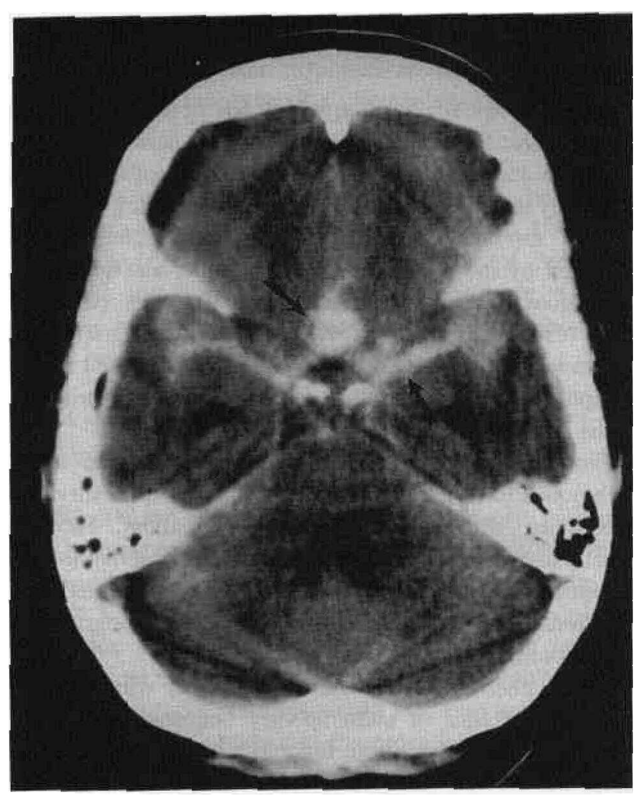

Figure 6-2 Ct of head without contrast showing a subarachnoid hemorrhage.

analyze the absorption of x-rays by all tissues to produce an :mage of high resolution in the transaxial (horizontal) plane.[2-3] At the present time, CT is readily available in most major hospitals, making it the most widely used neurodiagnostic modality. CT is accurate, fast, and well tolerated by patients—even those who have difficulty remaining motionless or who require life support systems.

The physical principle underlying the CT image is the same as in all radiography—the selective absorption of x-rays (photons) by tissues of different densities.[4] Tissues with greater density—for example, bone—will exhibit more absorption of the x-ray beam and will be displayed on the CT image as areas of high density (white). Tissues with less absorption (attenuation) of x-ray beams will be displayed as areas of lower density (varying shades of gray to black). Routine examinations of the brain with CT are performed with axial 10-mm slices through the entire brain and the base of the skull. Some specific anatomic regions—such as the posterior fossa, sella, orbits, temporal bone, or paranasal sinuses—can be evaluated with thinner sections in axial, axial oblique, and/or coronal imaging planes.

It is vital to recognize the advantages and limitations of CT relative to other imaging techniques such as MRI in the evaluation of intracranial pathology. Selection of the study of choice depends on multiple factors, such as history of acute or chronic trauma, the presence of cardiac pacemakers or metallic implants, the monitoring needs of the patients, or the presence of bone pathology versus soft tissue pathology. Generally, CT will be the initial study in patients presenting suspected intracranial hemorrhage that might be the result of head trauma, hypertension, or rupture of an aneurysm or infarction, as well as suspicion of intracranial tumors, either primary or metastatic.[5] CT of the head is the study of choice as well for evaluation of craniofacial trauma to include facial and skull base fractures. •

Thus, a nonenhanced CT of the head is recommended for evaluation of acute head trauma, subarachnoid hemorrhage (Fig. 6-2), acute stroke, follow-up of hydrocephalus or shunt malfunction, and for general evaluation of patients with dementia. A CT of the head should be obtained with intravenous contrast enhancement as a screening study for possible metastases, headaches of unknown etiology without neurological deficit, suspected aneurysms or vascular malformations, intracranial infections or abscess, or primary and metastatic brain tumors. CT supplemented by intrathecal contrast is excellent in evaluating CSF fistulas. CT of the head with 3-dimensional reconstruction is the study of choice preoperatively and postoperatively for evaluation of facial anomalies and craniosynostosis prior to surgery as well as for postsurgical evaluation.

Nevertheless, there are certain limitations of CT. Routine CT is suboptimal for evaluation of the prepontine and cerebellopontine angle cisterns unless special angulation is used and thin sections are obtained. This is due to the absorption of the x-ray beam by the thick petrous bones ("Hounsfield artifact"). The evaluation of the sellar region by CT should be performed in the coronal plane with intravenous contrast; however, the patient's position for the study may be awkward and uncomfortable, resulting in inconsistent image quality. Therefore, MRI is the study of choice for suspected lesions in the region of the sella.

INTRACRANIAL MAGNETIC RESONANCE IMAGING

The next major evolution in neuroimaging following CT in 1972 occurred with the clinical application of magnetic resonance imaging (MRI) in 1982.[6] MRI is a noninvasive computer-assisted imaging technique that differs from CT in the type of energy used. The MRI is based on measuring the phenomenon of *nuclear magnetic resonance* of the hydrogen atom in various tissues. Magnetic resonance imaging uses a strong magnetic field and the application of radiofrequency pulses to generate 2-dimensional or 3-dimensional images.

Nuclei of certain atoms, particularly hydrogen, respond to a strong magnetic field by aligning with or against the longitudinal axis of that magnetic field. This process is called *magnetization.* The number of hydrogen atoms aligned in the direction of the magnetic field is slightly greater than the number aligned against it, producing a net magnetization in the direction of the magnetic field. The magnitude of this net magnetization is related to the number of hydrogen nuclei in each volume of tissue *(proton density).* The direction of the net magnetization may be altered by the addition of energy in the form of a radiofrequency (RF) pulse of appropriate frequency.[7] This extra energy flips the magnetization vector away from its alignment with the primary magnetic field.

When the RF pulse is terminated, the hydrogen protons will begin to realign in the direction of the external magnetic field, releasing the excess energy initially used to deflect them from alignment. The rate at which this realignment occurs depends on the rate that the added energy is released to the surrounding environment. This process is called *longitudinal relaxation.* The time required for 63 percent of the magnetization vector to return to alignment with the external magnetic field is designated *Tl,* or *longitudinal relaxation time.*

A second component of relaxation occurs in the transverse plane around the axis of the magnetic field. The magnetization vector in the transverse plane is the sum of many nuclei rotating at slightly different frequencies, which are forced together by the application of the external RF pulse *(coherence).* The net magnitude of the transverse vector and its signal strength diminishes as the nuclei fan out within the transverse plane *(loose coherence).* The time required for 63 percent loss of the transverse coherence is designated 72, or *transverse relaxation time.* Different tissues will exhibit different Tl and T2 relaxation patterns, making their magnetic behavior different enough to be recognized as separate entities in the MR image.

The excess energy released by the protons as they realign with the magnetic field is radiated to the environment as a

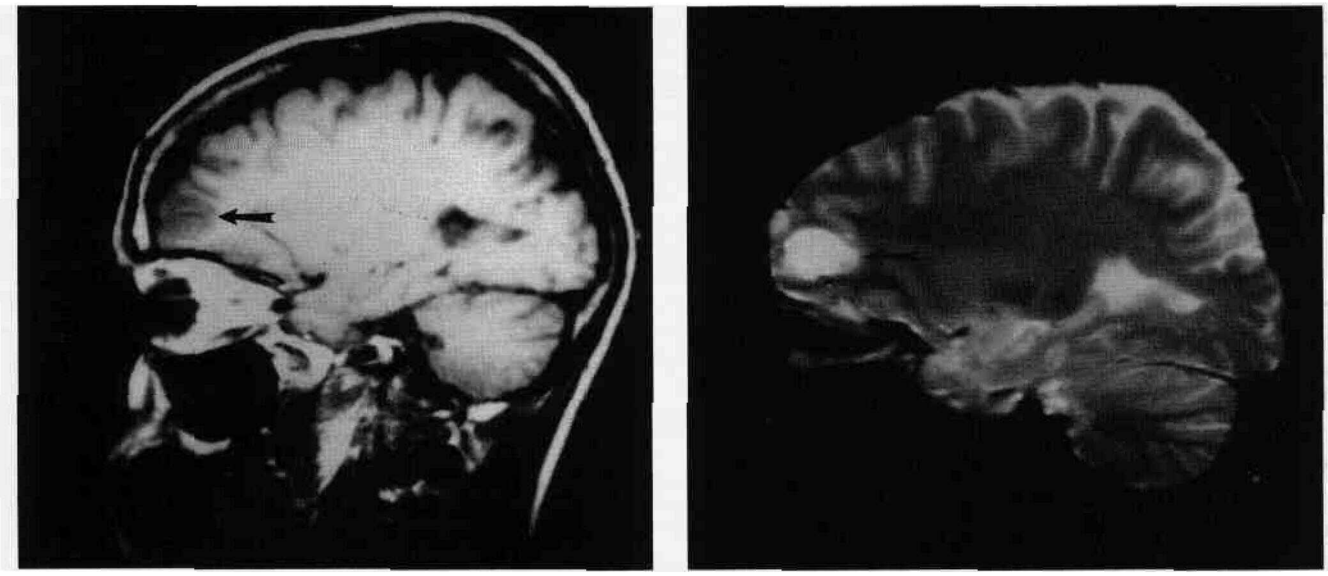

(A) (B)

Figure 6-3 MRI of cranium of a patient with astrocytoma. Sagittal Tl image to show MRI anatomic detail *(A).* Sagittal T2 image enhances visualization of lesion *(B).*

radio frequency "signal." The amount of signal *(signal intensity)* emitted per unit of volume will be correlated to a gray scale, where high signal intensity will be white and absence of signal will be black. The signal intensity of a tissue is related to its Tl and T2 relaxation times and its proton density.

MR images can be obtained in such a way as to favor the demonstration of structures with predominant Tl or with T2 characteristics. Tl-weighted images produce a strong MRI signal that results in anatomic images. In a Tl-weighted image, cerebrospinal fluid (CSF), cortical bone, air, and rapidly flowing blood will have negligible signals, appearing dark. The gray matter and white matter will Show different shades of gray, with the gray matter appearing slightly darker. Fat is intensely bright on Tl-weighted images, which is an advantage when outlining orbital fat or the epidural space or marrow in the spinal column. Subacute and chronic hematomas are seen as high signal intensity. The abundant signal of the Tl-weighted image is ideal for demonstrating detailed intracranial or spinal anatomy, for example, in evaluating the cerebellopontine angle cistern or the pituitary fossa. This is due to its high contrast between normal structures and the adjacent darker CSF. Tl-weighted images, however, are relatively insensitive to small changes in the water content of tissue. Therefore, small brain lesions that do not cause anatomic distortion are often invisible (Fig. 6-3).[8]

T2-weighted images are much more sensitive in the detection of small changes in the water content of the tissue examined.[11] Regions of increased water content *(edema)* are imaged as regions of high signal intensity superimposed on a darker background. Because of the lack of a strong background tissue signal, T2-weighted images do not display the anatomy as sharply as the Tl-weighted image does. Nevertheless, the high sensitivity of T2-weighted images for the detection of changes in tissue water content is the primary reason for the increased sensitivity of MRI over CT in the detection of brain and spinal cord pathology. In T2-weighted images, the dominant tissue producing the highest signal intensity will be bulk water, making CSF the dominant bright signal factor in comparison to gray and white matter. Cortical bone, air, and rapidly flowing blood still present negligible signals (black). Fat in T2-weighted images presents lower signal intensity than in Tl-weighted images. Areas of demyelination, edema, infarction, or tumor infiltration will have higher water content (more hydrogen atoms) and will produce higher signal intensities than the surrounding tissues.

A definite advantage of MRI over all other imaging modalities is its ability to image multiple direct planes (axial, sagittal, coronal, or any degree of oblique projections) without a change in the patient's supine position. The absence of signal from surrounding bone allows excellent anatomic detail of structures adjacent to bone, both intracranially and throughout the spinal canal. Most MRI examinations of the brain include sagittal, coronal, and axial projections. The axial images are most commonly obtained to evaluate the brain. The coronal images are most useful in evaluating sellar and parasellar regions. With both, the axial or the coronal images, side-to-side comparison is possible. Direct sagittal images are extremely useful when evaluating midline pathology of the brain, such as sellar tumors, pineal masses, brainstem tumors, vermian atrophy, obstructive hydrocephalus, or congenital malformations. They are also helpful in visualizing the location of other internal pathology in the lateral view (Fig. 6-4).

Gadolinium (Gd), a heavy rare-earth element, is being used in special solutions as the intravenous contrast agent for MRI of the central nervous system (CNS).[10] Although free Gd is toxic, its compound chelated to diethylenetriamine

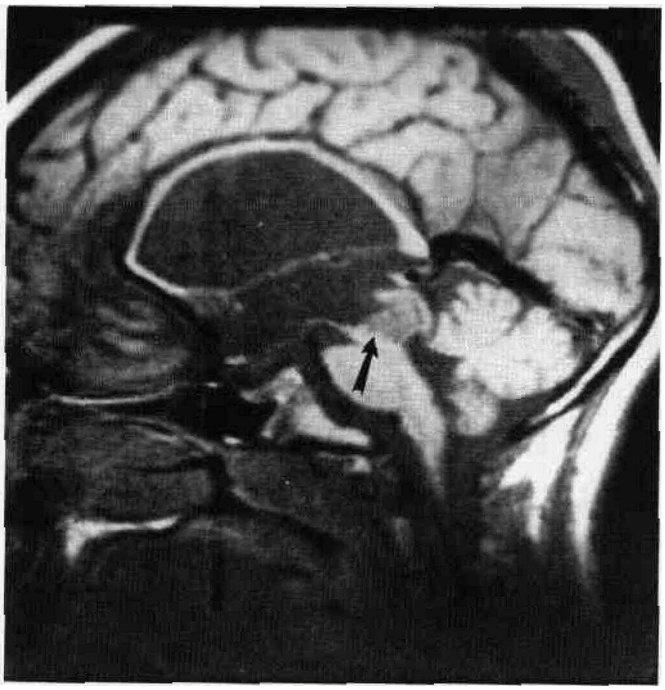

(A)

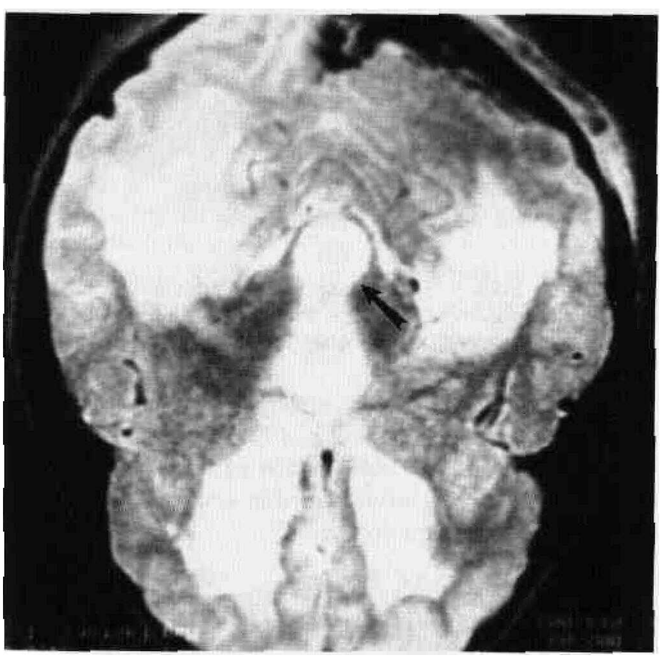

(B)

Figure 6-4 MRI of cranium showing midbrain tumor and hydrocephalus. Sagittal Tl image shows aqucductal obstruction by tumor *(A)*. Axial T2 image shows tumor involvement *(B)*.

pentaacetic acid (DTPA) or other chelating agents exhibits "paramagnetic behavior." When deposited within tissue, this compound greatly decreases the Tl relaxation time of the surrounding tissue, resulting in a high signal intensity on Tl-weighted images. Because of the nature of the blood-brain barrier, Gd will only move outside of the intravascular space in areas of absence or breakdown of the blood-brain barrier. Damage to the blood-brain barrier is a nonspecific alteration that occurs with pathology within the brain, as seen with tumors, infection, and infarction. Gadolinium-DTPA, the current agent employed for contrast MRI, has been shown to be safe, with very few reported allergic reactions in over 5 million administered doses. The use of paramagnetic contrast increases the sensitivity of MRI for detection of specific disease processes, particularly small tumors. The pattern of contrast enhancement in MRI allows for better tissue characterization of the visualized lesions. Pituitary gland, infundibulum, choroid plexus, pineal gland, and dural reflections lack a blood-brain barrier and will normally enhance with Gd. Slowly flowing blood within the cavernous sinus or in the cortical veins will also exhibit normal enhancement (Fig. 6-5).

Contraindications to MRI include the presence of ferromagnetic materials in soft tissues of the body, such as old intracranial aneurysm clips or intraocular metallic foreign bodies that could move in the fluctuating magnetic field and damage structures on which they are located." Contraindications also include such devices as cardiac pacemakers that could malfunction in the magnetic field or large metallic implants that may become heated by magnetic induction.[12] Since the effect of high magnetic fields and radiofrequency energy on fetuses has not been determined, pregnant patients are generally excluded at the present time. Patients with claustrophobia may not be able to remain in the MR unit for the required time. Quality MRIs require patients to remain motionless for 10 to 15 min. The magnetic environment restricts the use of conventional electronic monitoring devices. Therefore, critical or unstable patients are difficult to monitor and require special attention or equipment while undergoing MRI.

MRI is most sensitive in detection of pathology in the CNS, except for evaluation of acute intracranial hemorrhage or parenchymal calcifications.[13] MRI is rapidly becoming the study of choice in many other conditions that affect the brain, the reason being the absence of artifacts from bony structures surrounding the brain, especially in the posterior fossa (Fig. 6-6). Also, MRI has the capability of acquiring multiplanar images without the need for manipulation of position of the patient, which is especially useful for evaluation within or around the pituitary fossa. Nonenhanced MRI of the brain is useful for screening demyelinating diseases like multiple sclerosis (Fig. 6-7), ischemic brain disease, dementia, and for primary evaluation of the etiology and site of obstruction in hydrocephalus. MRI of the brain is also routinely used to diagnose tumors in pediatric patients. It is the study of choice in the evaluation of congenital anomalies of the CNS, such as agenesis of the corpus collosum (Fig. 6-8), Chiari malformations, migrational anomalies, schizencephaly, problems of brain maturation, or pediatric vascular accidents and vascular malformations.

Recent advances in MRI include magnetic resonance angiography (MRA) and magnetic resonance spectroscopy. MRA has the potential to replace routine angiography for screening of disease at the carotid bifurcation (Fig. 6-9). Its potential in the evaluation of intracranial vascular

(A)

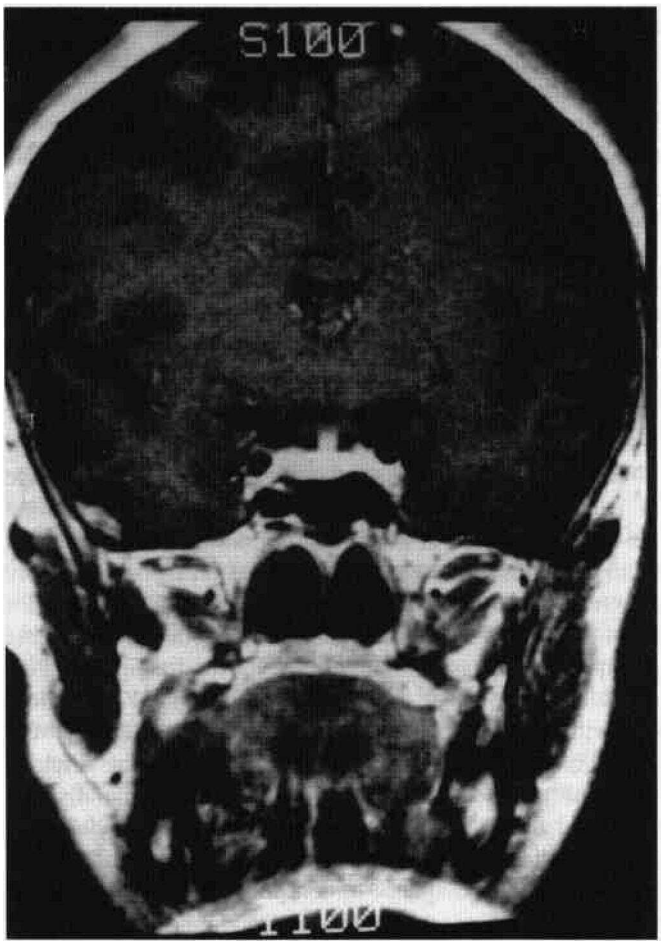

(B)

Figure 6-5 MRI of normal cranium after administration of gadolinium. Midline sagittal enhancement *(A).* Coronal sella enhancement *(B).*

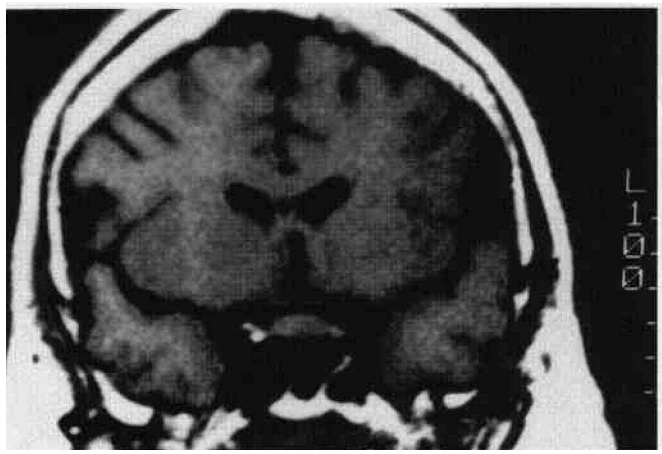

(A)

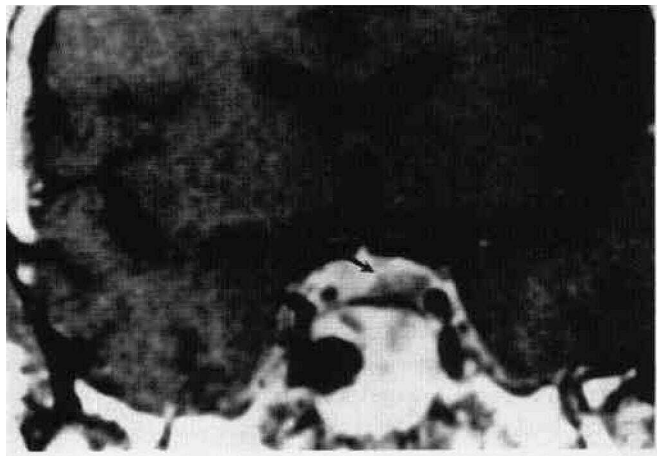

(B)

Figure *6-6* MRI of cranium demonstrating pituitary microadenoma. Coronal Tl image without Gd *(A).* Coronal Tl image with Gd, showing lesion *(B).*

malformations and occlusive vascular disease (for example, moyamoya disease) is being explored.[14] MR spectroscopy may provide information on the metabolic status of different areas within the brain and may be helpful in the evaluation of patients with temporal lobe epilepsy, Alzheimer's disease, brain tumors, and determination of brain death.[15] The selection of MRI, CT, or a combination of these examinations depends on the kind of information sought and the time needed to acquire that information.

CEREBRAL ANGIOGRAPHY

The radiographic demonstration of the vasculature of the head and neck using an intraarterial contrast media was first described by Moniz in 1927.[16] Initially, the morbidity associated with this procedure was high, owing to the techniques employed and the toxicity of the contrast media. In 1944, Engeset reported 100 cases using a carotid cannulation technique with relatively low morbidity.[17] Less-toxic contrast media were developed and the technique gained widespread acceptance by the late 1940s. In 1953, Seldinger described a technique for femoral artery cannulation and selective arterial injection, further enhancing the diagnostic capabilities and relative safety of cerebral angiography.[18]

From the early 1950s until the early 1970s, cerebral

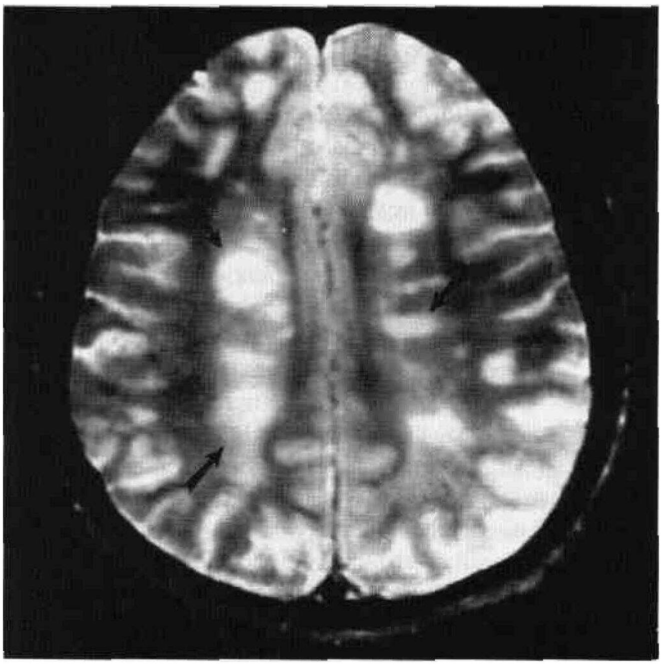

Figure 6-7 MRI of cranium of patient with multiple sclerosis. Axial T2 image showing paraventricular lesions.

angiography in tandem with pneumoencephalography was the mainstay of diagnostic cranial neuroradiology. With the advent of CT scanning in the early 1970s, the use of angiography was significantly curtailed, particularly for evaluating trauma.[5] The evolution of third- and fourth-generation CT scanners and the incorporation of MRI into the diagnostic armamentarium have resulted in the elimination of many of the diagnostic applications of cerebral arteriography.

At facilities where high-quality CT imaging and MRI are available, indications for cerebral angiography are usually limited to the following:

1. Demonstration of the vascular supply of tumors or demonstration of the relationships of major arteries or veins to tumors.

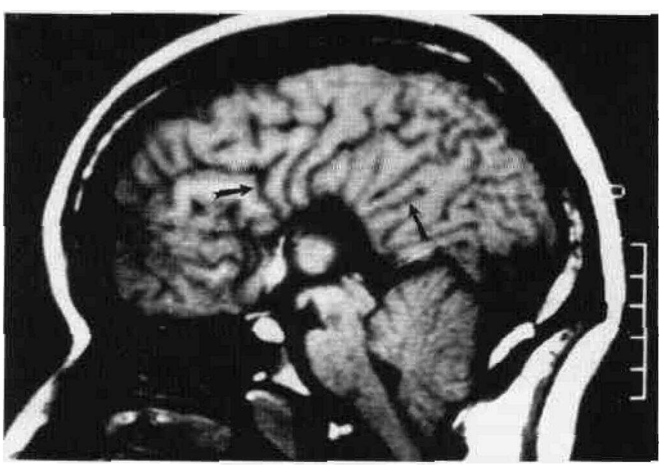

Figure 6-8 MRI of cranium demonstrating agenesis of corpus callosum. Sagittal Tl image.

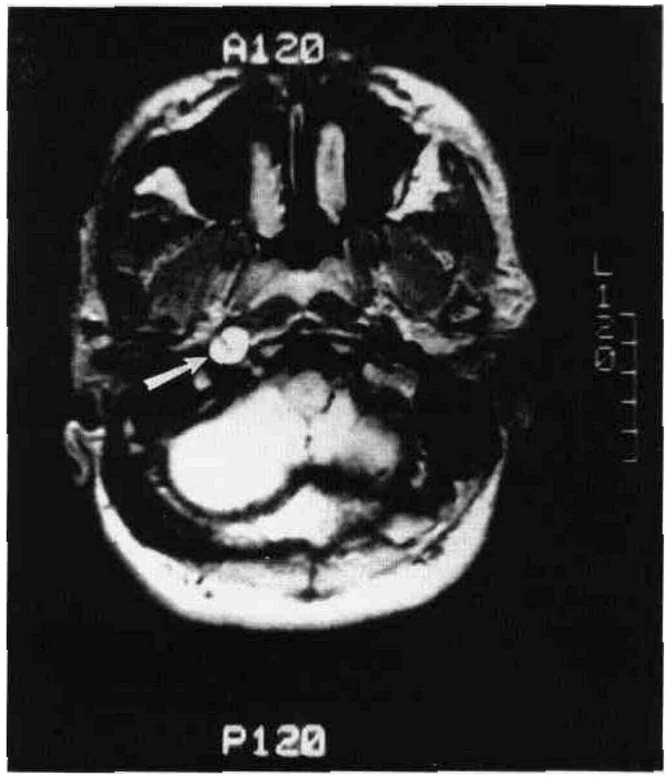

Figure 6-9 MRI/angiogram demonstrating carotid dissection. Magnetic resonance angiography.

2. Evaluation of cerebrovascular lesions such as arteriovenous malformations (AVM), aneurysms, arteriosclerosis, or arteritis.
3. Specialized studies such as Wada testing for hemispheric dominance.
4. Endovascular embolization procedures.

Contemporary cerebral angiography employs electronic digital imaging with computerized subtraction and/or biplanar arteriography and fluoroscopy, an automatic contrast injector, and automatic film changers. The Seldinger technique, or a modification thereof, in most cases provides the safest means of selective arterial injection; however, on rare occasions a retrograde brachial or direct carotid injection may be necessary to obtain a complete study.[18]

Physicians requesting or performing cerebral angiography should be familiar with the normal cerebrovascular anatomy. commonly occurring anatomical variations, and typical angiographic patterns, as well as appearance of various lesions.

Aortic Arch The *aortic arch* study is traditionally part of the standard cerebral angiogram. Currently, many institutions perform this study using digital subtraction angiography (DSA) in an effort to reduce the total amount of contrast media. The study is usually obtained in right posterior oblique (RPO) and left posterior oblique (LPO) projections. These views are important in the evaluation of ischemic cerebrovascular disease, since lesions or anomalous vascular origins in the region of the aortic arch may have an impact on treatment planning (Fig. 6-10).

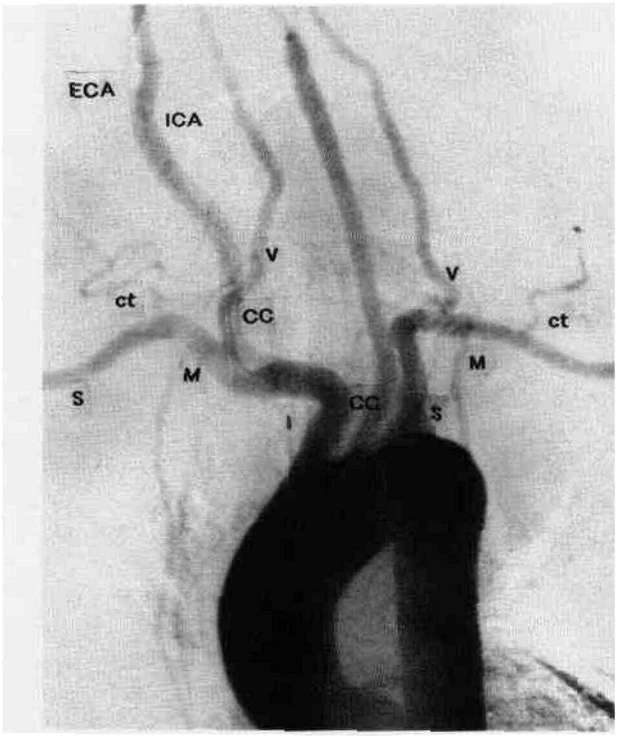

Figure 6-10 Angiogram of the aorlic arch. I = innominate; M = mammary; S = subclavian; CC = common carotid; V = vertebral; EGA = external carotid artery; ct = thyrocervical trunk; ICA = internal carotid artery.

The innominate artery is the most proximal major branch of the aortic arch. This vessel divides into the right subclavian and right common carotid arteries. The right vertebral artery typically arises from the right subclavian artery within a couple of centimeters of its origin. On rare occasions an aberrant right subclavian artery may arise from 3ie posterior wall of the aortic arch at or just distal to the origin of the left subclavian artery.

The left common carotid artery usually arises as a separate branch of the aortic arch just distal to the origin of the innominate artery, although these arteries may share a common origin. The left subclavian artery consistently arises from the anterosuperior surface of the aortic arch distal to the left common carotid origin and almost immediately gives rise to the left vertebral artery. Occasionally, the left vertebral artery will originate directly from the aortic arch between the origin of the left common carotid artery and the left subclavian artery. The left vertebral artery is typically the dominant vertebral artery and is therefore the preferred vessel for injection in the performance of posterior fossa angiography.

Carotid Artery The *common carotid artery* arises from the innominate artery or the aortic arch and usually has no major branches until its bifurcation into internal and external carotid arteries in the midcervical region. The bulbous-shaped bifurcation is the most common site of origin of atherosclerotic plaques that extend into the internal and external carotid arteries for varying distances, creating turbulence and obstruction to blood flow (Fig. 6-11).

External Carotid Artery The *external carotid artery* is most often found anteromedial to the internal carotid artery and is normally the smaller of the two vessels. Of the seven to eight branches that arise from the external carotid artery, the internal maxillary, the major terminal branch, is of principal importance in neuroradiology. This artery gives rise to the middle meningeal artery, which enters the base of the skull via the foramen spinosum and provides blood supply to the dura over the sphenoid wing and over the frontal and parietal lobes. The meningeal arteries and their branches enlarge to supply meningeal tumors or dural arteriovenous malformations in this region. Terminal branches of the internal maxillary artery anastomose with distal branches of the ophthalmic artery, thus providing an important avenue of collateral blood flow to the intracranial arterial circulation. This is most commonly demonstrated after complete occlusion of the internal carotid artery proximal to

Figure 6-11 Arteriogram. Lateral view of extracranial carotid artery. CC = common carotid; ICA = internal carotid artery; EGA = external carotid artery; I = superior thyroid; L = lingual; F = facial; O = occipital; M = maxillary; STA = superficial temporal; arrow = catheter tip.

the supraclinoid segment. These vessels may also enlarge to supply ineningeal tumors in the region of the sphenoid planum or olfactory groove. In cases of arteritis, the terminal branches of the external carotid artery frequently demonstrate typical angiographic patterns of this disease.

Internal Carotid Artery The *internal carotid artery* may be divided into four anatomical segments: cervical, petrous, cavernous, and supraclinoid. The cervical segment has few angiographically demonstrable branches except when there is persistence of a primitive hypoglossal artery. When present, this vessel arises from the cervical segment and ascends through the hypoglossal canal to anastomose with the basilar artery in the posterior fossa. Similarly, the petrous segment has few branches of angiographic significance save for the rare occurrence of a persistent primitive acoustic artery anastomosing with the basilar artery of the posterior circulation. Occasionally, a caroticotympanic branch feeds a glomus tumor in this region.

The cavernous segment of the internal carotid artery sometimes gives rise to a persistent trigeminal (mesencephalic) artery connecting the anterior and posterior circulations. This anomaly may be associated with an atretic posterior communicating artery, an atretic anterior cerebral artery, or an intracranial aneurysm. The cavernous segment also gives rise to a meningohypophyseal artery, which divides into the meningeal artery, supplying the tentorium and the inferior hypophyseal arteries. The meningeal artery, the artery of Bernasconi and Casanori, is rarely apparent except in association with a meningioma of the clivus or the tentorium or with a local dural arteriovenus malformation (AVM).

The supraclinoid segment gives rise to three major branches, the ophthalmic, the posterior communicating, and the anterior choroidal arteries, prior to its terminal bifurcation into the anterior and middle cerebral arteries (Fig. 6-12). The ophthalmic artery arises from the ventral surface of the internal carotid artery as it exits the cavernous sinus. From the initial segment of the ophthalmic artery originate a number of small arteries (ethmoidals), which supply the ethmoid sinuses and the dura overlying the sphenoid planum and floor of the frontal fossa. These arteries become prominent in the presence of meningeal tumors of the region. A recurrent meningeal artery may arise from the ophthalmic artery, and rarely this vessel gives rise to the middle meningeal artery. The terminal branch of the ophthalmic artery is the retinal artery. Angiograms outlining the retinal artery often demonstrate a choroidal blush of the posterior globe.

The posterior communicating cerebral artery (PComA) arises from the posterior wall of the supraclinoid internal carotid artery and courses posteromedially to join the posterior cerebral artery (PCA). The branch point of the PComA from the internal carotid artery is one of the most common sites of occurrence of a saccular (berry) aneurysm. The artery may be atretic. Rarely, there may be "fetal origin" of the PCA, where it arises directly from the supraclinoid ICA without an intervening PComA, in which case there is no communication with the basilar artery.

The anterior choroidal artery arises from the intracranial carotid artery just distal to the PComA. This point of branching is another common site for a saccular aneurysm The anterior choroidal artery initially courses posteromedially and ultimately turns superolateral to enter the choroidal fissure and supply the choroid plexus of the temporal lobe.

The intracranial carotid artery terminates by bifurcating into the anterior and middle cerebral arteries.

The initial segment of the anterior cerebral artery (ACA) complex courses anteromedially from the bifurcation, beneath the orbital portion of the frontal lobe and turns superiorly in the cistern of the lamina terminalis. Here, it gives rise to a short segment, the anterior communicating artery (AComA), which anastomoses with the opposite anterior cerebral artery. The segment from the bifurcation of the intracranial carotid artery to the anterior communicating artery is often referred to as the *A-l segment.* The segment of anterior cerebral artery beyond the origin of the anterior communicating artery is referred to as the *A-2 segment* and gives rise to one or two small lenticular branches, the larger of which is usually called the "recurrent artery of Huebner." The region around the AComA is where most saccular aneurysms of the ACA occur. Beyond this point, the distal anterior cerebral artery, which is also known as the "pericallosal artery," gives rise to the frontopolar branch and proceeds superiorly and posteriorly above the genu and over the superior surface of the corpus callosum. The artery terminates in a number of callossomarginal branches and the artery of the pericallosal sulcus.

The middle cerebral artery, as it originates from the bifurcation of the intracranial carotid artery, courses slightly anteriorly and superiorly and then becomes almost horizontal as it courses laterally toward the sylvian fissure. This horizontal segment gives rise to a number of small lenticulostriate vessels, which are barely demonstrable on angiography, followed by major branches to supply the frontal and/or anterior temporal lobes. The segment of the middle cerebral artery proximal to its turn (genu) into the sylvian fissure is referred to as the *M-l segment.* From the genu, the artery courses posteriorly and superiorly in the sylvian fissure, typically giving rise to two or three major branches, referred to as the *bifurcation* or *trifurcation.* Any of these branch points may be the sites of saccular aneurysms; the trifurcation is the most common site for aneurysms of the middle cerebral artery. Distally, branches of the middle cerebral artery extend over the surface of the frontal, temporal, and parietal lobes. Other major branches, deep in the sylvian fissure loop over the insular cortex, the island of Reil. Viewing the angiogram made in the AP projection, the terminal loop of middle cerebral artery most posterior and medial is referred to as the *sylvian point.* Viewing the lateral projection, the sylvian point is again identified as the most distal point of the terminal loop of the middle cerebral artery. A triangle may be constructed by drawing a line from the sylvian point to the genu of the middle cerebral artery, and another line from the sylvian point tangential to the

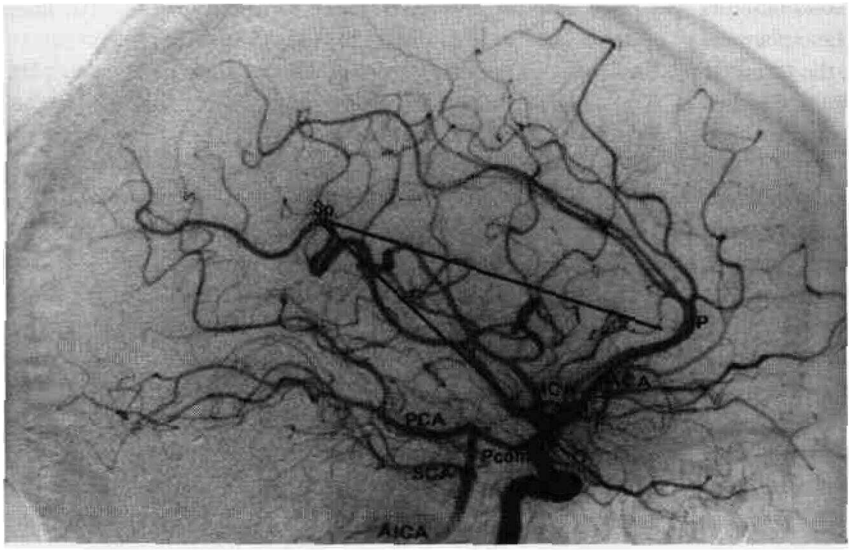

(A)

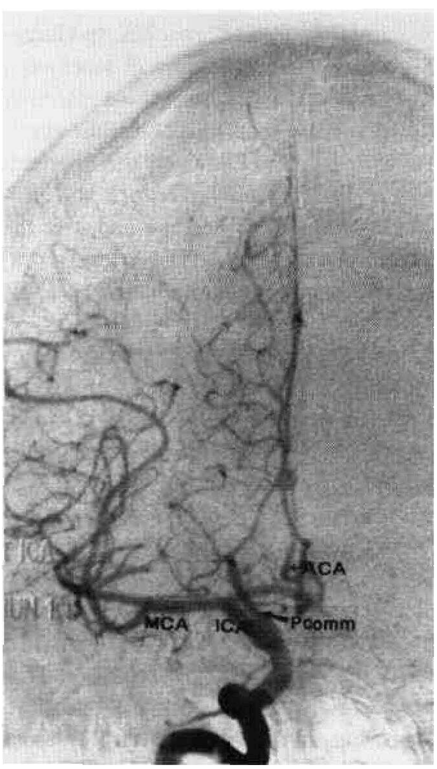

(B)

Figure 6-12 Normal carotid angiogram demonstrating primitive-type posterior communicating artery (Pcom) with filling of the right anterior and entire posterior circulation. Note also the well-defined sylvian point (Sp) and outline of the sylvian triangle. Lateral projection carotid angiogram *(A).* AP projection carotid angiogram *(B).* MCA = middle cerebral artery; ACA = anterior cerebral artery; O = ophthalmic; PCA = posterior cerebral artery; F = frontopolar; P = pericallosal; SCA = superior cerebellar artery; AICA = anterior inferior cerebellar artery.

middle cerebral artery loops over the insular cortex to the level of the carotid bifurcation (Fig. 6-12). These two landmarks, the sylvian point and the sylvian triangle, are useful in locating intracranial masses by cerebral angiography.

Posterior Circulation Other than the exceptions of aberrant circulation previously noted, the posterior cerebral circulation is supplied principally by the vertebral arteries and a variable contribution from the posterior communicating arteries. The vertebral arteries enter the skull through the foramen magnum posterolateral to the brainstem. At approximately the level of the caudal pons, they course ventromedially and join in the midline to form the basilar artery. Prior to this junction, each vertebral artery gives rise to a posterior inferior cerebellar artery (PICA). Aneurysms of the posterior circulation commonly occur where the PICAs branch from the vertebral arteries. Each PICA has two major branches: a tonsillohemispheric branch with a caudal loop which passes around the lowest extent of the cerebellar tonsils prior to terminating over the posteroinferior aspect of the cerebellar hemisphere and a terminal vermian branch which approaches the midline (Fig. 6-13). The caudal drop of the tonsillo-

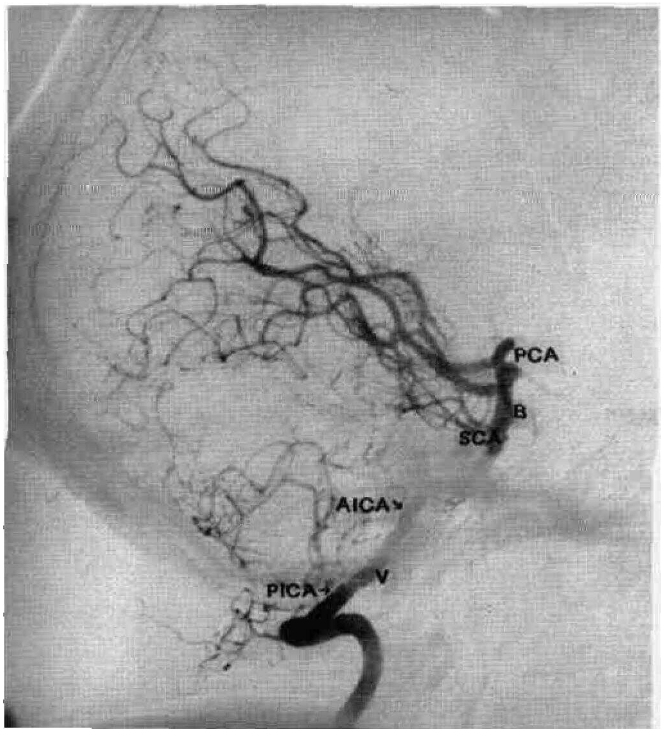

(A)

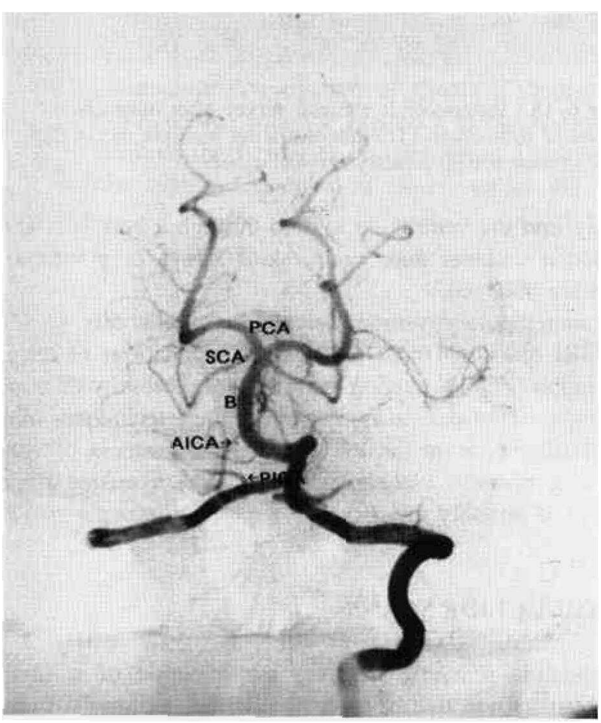

(B)

Figure 6-13 Normal vertebral angiogram. Lateral *(A)* and AP projection *(B)*. V = vertebral; PICA = posterior inferior cerebellar artery; AICA = anterior inferior cerebellar artery; B = basilar artery; SCA = superior cerebellar artery; PCA = posterior cerebral artery.

hemispheric artery is useful in identifying caudal descent of the cerebellar tonsils through the foramen magnum, as may **be** seen in tonsillar herniation and Chiari malformations. The vermian branch may be helpful in Moralizing intraaxial posterior fossa tumors.

The first major branch of the basilar artery is the anterior inferior cerebellar artery (AICA), which courses laterally around the pons to become adjacent to the seventh and eighth cranial nerves. It then continues laterally over the ventrolateral surface of the cerebellar hemisphere. This vessel is frequently elevated by tumors in the region of the cerebellopontine angle; it is occasionally the site of aneurysms or may supply arteriovenous malformations.

The superior cerebellar arteries arise as paired branches from the distal basilar artery and course laterally around the brainstem in the ambient cistern and then superiorly over the surface of the cerebellum beneath the tentorium. The origin of *these vessels is infrequently the site of aneurysms. The* vessels may supply AVMs or tumors. Their initial segments may be displaced upward or downward by transtentorial herniation.

The large paired posterior cerebral arteries are the terminal branches of the basilar artery. Basilar tip aneurysms occur at the branching point. The posterior cerebral artery courses around the midbrain above cranial nerve III and becomes supratentorial. The artery then divides and gives off branches posteriorly, superomedially, and laterally.

Cerebral Veins The cerebral venous drainage may be divided into superficial and deep venous systems. The superficial venous system is primarily composed of veins that overlie the gyral surfaces and drain into major venous sinuses. The deep venous system, for angiographic purposes, includes the paired internal cerebral veins and the deep medullary veins, which ultimately drain into the vein of Galen and the straight sinus (Fig. 6-14).

Lesions overlying the surface of the brain, such as subdural or epidural hematomas, visibly displace the superficial cerebral veins away from the inner table of the skull. Deeper lesions, within the brain substance, displace the deep veins with reference to the midline. Other lesions demonstrated by venous angiography include the early draining veins of a neoplasm or vascular malformation or venous sinus occlusion. The sequence and timing of venous drainage may also be helpful in identifying such signs as the early draining vein of a neoplasm or vascular malformation or a venous sinus occlusion or thrombosis.

ENCEPHALOGRAPHY

Encephalography, which encompasses pneumoencephalography and ventriculography, was described by Walter Dandy in 1918 and is one of the oldest neuroradiological imaging techniques.[19] By convention, encephalography combines the use of plain skull x-rays or polytomograms with the use of air or other radiographic contrast media injected into the ventricular or subarachnoid spaces of the brain.[20] In pneumoencephalography, air is injected into the subarachnoid space via a lumbar or cisternal puncture and subsequently

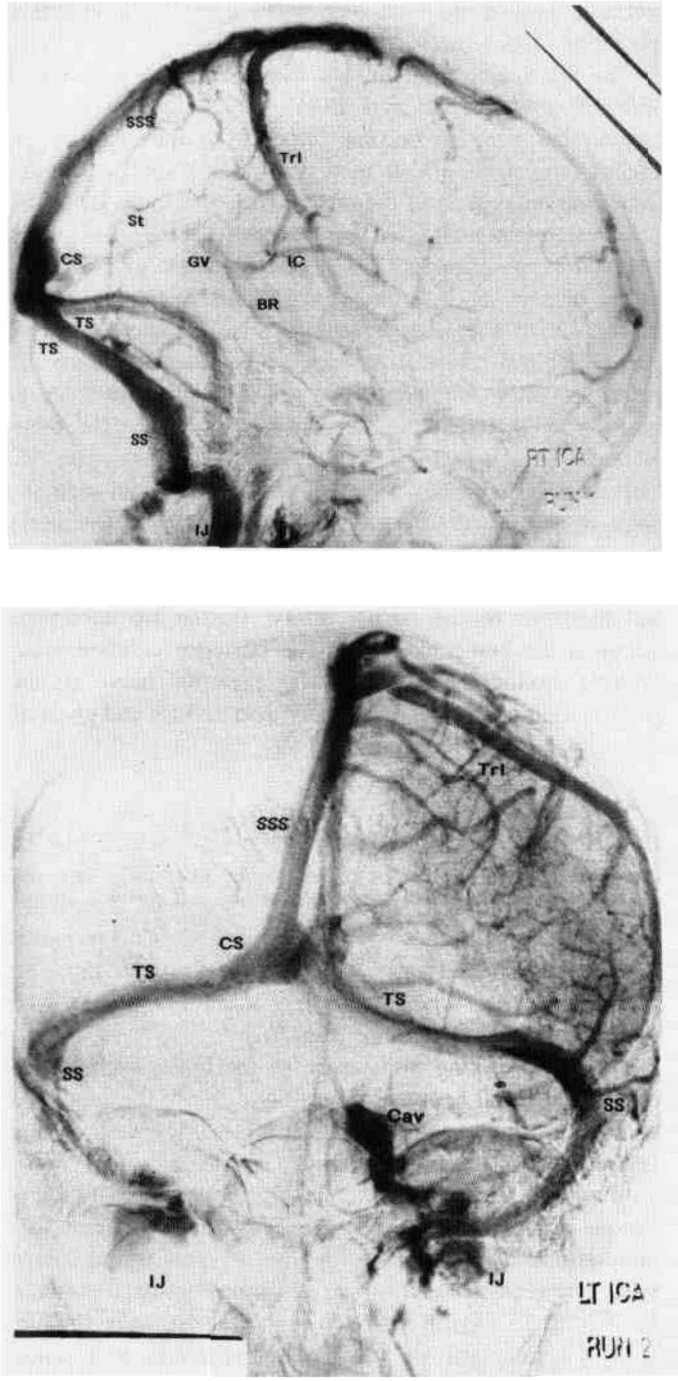

(B)

Figure 6-14 Normal venous phase of carotid angiogram. Lateral *(A)* and AP *(B)* projection of venous phase.
IJ = internal jugular; SS = sigmoid sinus; SSS = superior sagittal sinus; St = straight sinus; TS = transverse sinus; Trl = trolardi vein; CS = confluence of sinuses; Cav = cavernous sinus; GV = great vein of Galen; BR = basal vein of Rosenthal; 1C = internal cerebral vein.

skull x-rays or polytomograms obtained in various projections, while manipulating the position of the patient to accomplish movement of the air throughout the ventricular and cisternal systems.

In ventriculography, air or other contrast media is injected directly into the ventricular system through a burr hole and ventricular catheter and, again, skull x-rays or polytomograms are obtained.[21]

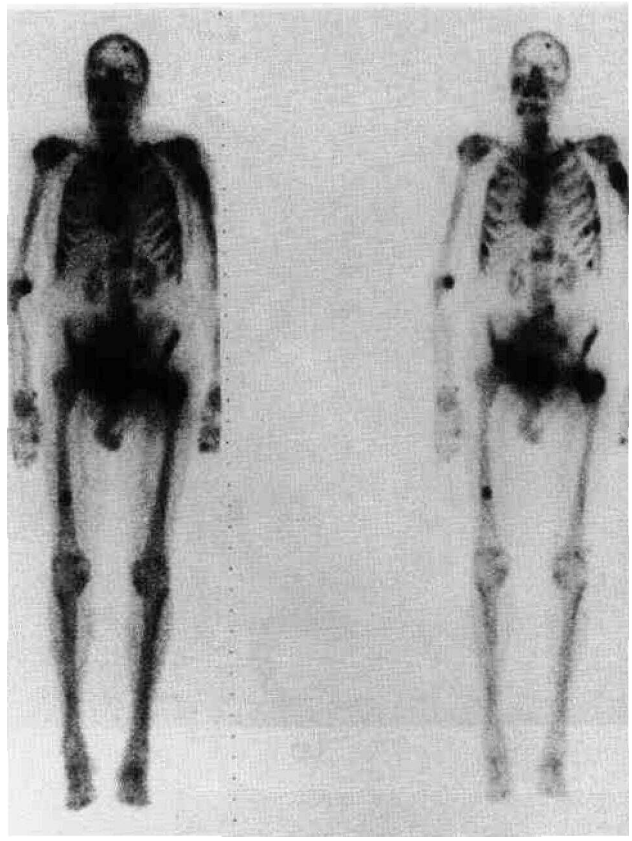

Figure 6-15 Radionuclide skeletal survey after intravenous injection of technetium (Tc) demonstrating multiple metastatic lesions in patient with primary cervical cancer.

In contemporary neuroradiology, the availability of CT and MRI has supplanted the general applications of encephalography and eliminated the attendant morbidity of these procedures. The specific application of these techniques may be expeditious, as in the intraoperative assessment of ventricular or cisternal catheter position or the assessment and removal of pituitary tumors.

RADIONUCLIDE SCANS

Radionuclide scanning involves the injection of a small amount of radioactive isotope, usually technetium (Tc) into the blood or cerebrospinal fluid (CSF).[22] The location and relative activity of the isotope is subsequently detected at various time intervals by a scintillation camera or a series of scintillation detectors. CT scanning and MRI have replaced radionuclide scanning for many applications. Remaining applications include: (1) skeletal surveys for metastatic disease or infection (Fig. 6-15); (2) cranial surveys (cisternography) for CSF fistulae (Fig. 6-16); (3) radionuclide angiography, which provides physiological information related to cerebral blood flow and compensated collateral flow (Fig. 6-17); and

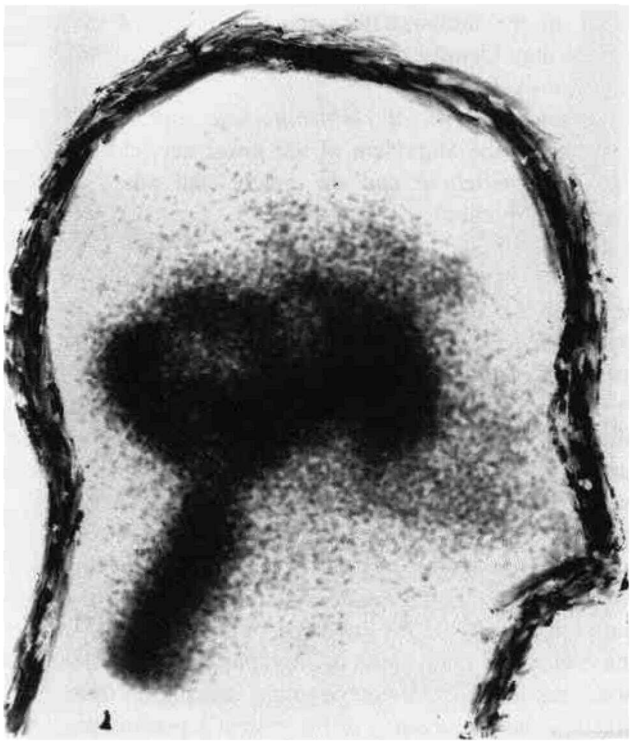

Figure 6-16 Radionuclide cisternogram using indium to demonstrate anterior fossa CSF fistula.

(4) radionuclide investigation of shunts ("shunt-o-grams") which may demonstrate the existence of obstruction to CSF flow between the ventricles or subarachnoid spaces and the recipient cavity. Examples of these studies are provided below.

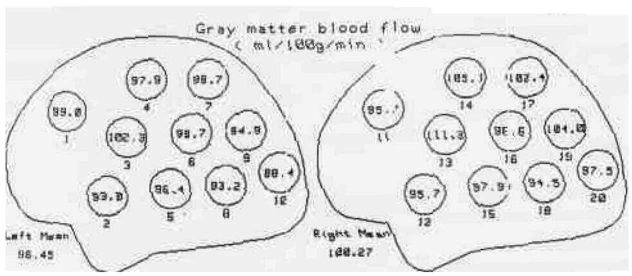

(A)

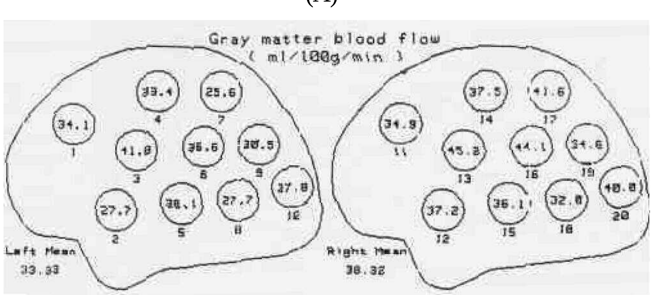

(B)

Figure 6-17 Regional cerebral blood flow scans. Computer-generated scintigraphs of normal xenon (Xe) uptake over various brain regions *(A)*. Computer-generated scintograph demonstrating diffuse cerebral hypoperfusion *(B)*.

POSITRON EMISSION COMPUTED TOMOGRAPHY (PET)

PET employs the use of positron emission radionuclides attached to metabolites, typically glucose. After intravenous administration, these radionuclides are detected by specialized scanning devices, similar to the scintillation detectors used in traditional radionuclide scanning. The major advantage of this technique is that it provides images that reflect physiological information, specifically the relative increase or decrease in the activity of the positron-tagged metabolite in the brain.[23] The major disadvantages are the enormous expense of acquiring and maintaining a cyclotron to generate the positrons and the rather limited clinical applications.

NEURORADIOLOGY OF THE SPINE

PLAIN SPINE RADIOGRAPHY

Plain radiographs of the spine are still the first imaging studies obtained in the evaluation of patients with suspected spinal disease or injury. Portable radiographs of the spine may be performed on site, with a minimum of patient manipulation. More extensive protocols involving multiple views and patient manipulation may be employed in an effort to define more clearly the anatomy of bones and joints. The major failing of plain spine radiography is its inability to image adequately noncalcified tissue intimately related to the spine, such as the spinal cord, intervertebral disks, and adjacent soft tissues. The most important observations made from plain spine radiographs relate to the structural integrity of the spinal column and the adequacy of the spinal canal. The most useful views for this purpose are the following:

Lateral projection. Demonstrates the anterior-posterior diameter of the canal, the alignment and regional contour of the spine, the height and shape of the vertebral bodies and disk spaces, the joint spacing and continuity of the posterior elements, and the relationship of the atlas and axis at the craniovertebral junction (Fig. 6-18).

Lateral views. May also be obtained with the patient in flexion and extension to aid in the assessment of structural integrity (Fig. 6-19).

Anteroposterior projections. Demonstrate the interpedicular distance or coronal diameter of the spinal canal, the shape and thickness of the pedicles, and the presence of dysraphic lesions or soft tissue masses (Fig. 6-20).

Additional projections may include the following:

Open mouth views of the odontoid. Used to assess the integrity and continuity of the dens and its relationship to the lateral masses of the atlas (Fig. 6-21).

Figure 6-18 Normal lateral projection of cervical spine.

Oblique views. Used to assess the pedicles, neural foramina, lamina, and articular pillars and joint spaces.

Anteroposterior pelvic views. Demonstrate the relationship of the lumbosacral spine to the rest of the pelvis. They may identify pelvic fractures associated with neurological dysfunction.

Swimmers' views of cervicothoracic junction. Used to determine the alignment of the lower cervical and upper thoracic vertebrae and the height and shape of these vertebral bodies.

In practice, a complete spinal survey employing all of the views described above in each region of the spine is rarely required. The extent and direction of the radiographic examination is usually determined from the information obtained through the history and physical examination, with historical information often being the major determinant. Consequently, the judgment of what constitutes an adequate examination varies. In the situation presented by an unconscious trauma victim with an apparent paraparesis, the radiographic examination may be extensive, whereas the evaluation of subacute neck pain with a discrete radiculopathy may forego plain spine radiography in favor of myelography or MRI. The efficacy of plain spine radiography will vary, depending on die nature of the lesion or injury, the region of the spine affected, and the urgency of the patient's presentation.

In general, nonskeletal lesions and lesions with extraskeletal extension—such as neoplasms, infectious processes, vascular malformations, herniated intervertebral disks, and some congenital malformations—are rarely adequately iden-

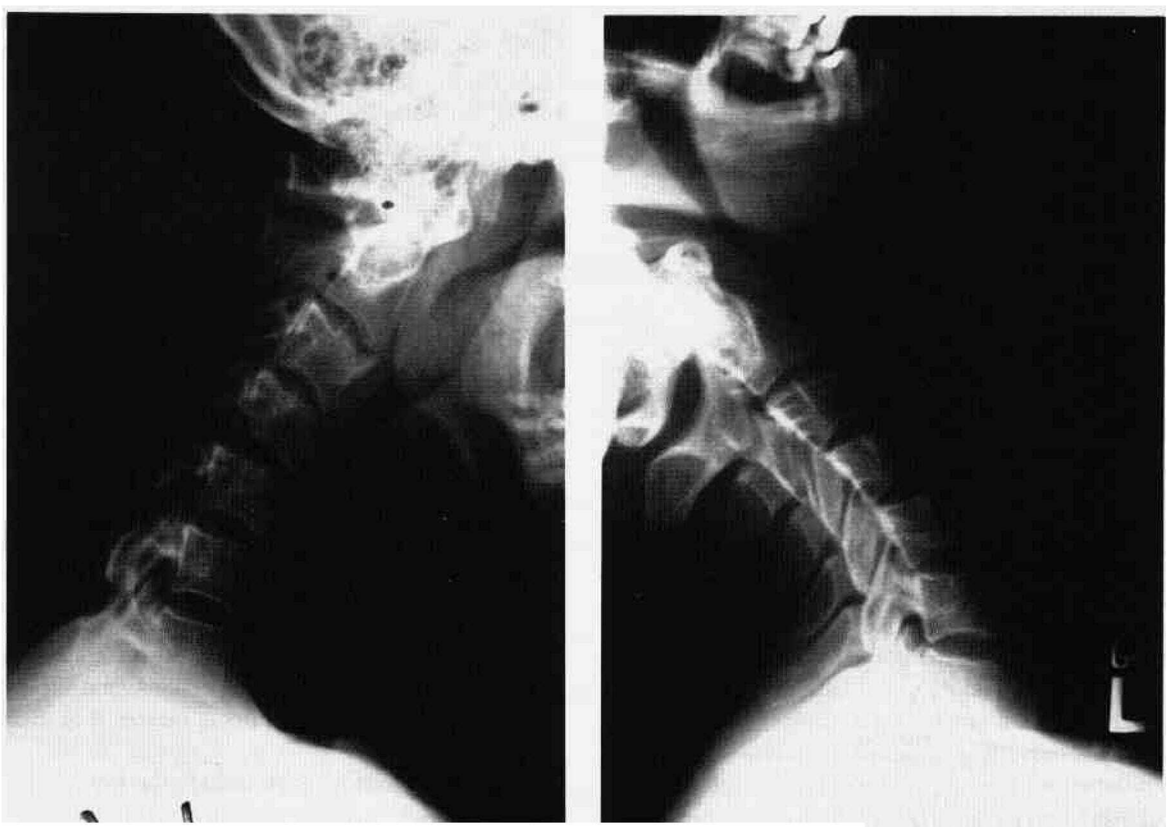

(A) (B)

Figure 6-19 X-ray of cervical spine in extreme flexion and extension. Note the even distribution of movement over all motion segments. Lateral cervical spine in extreme flexion *(A).* Lateral cervical spine in extreme extension *(B).*

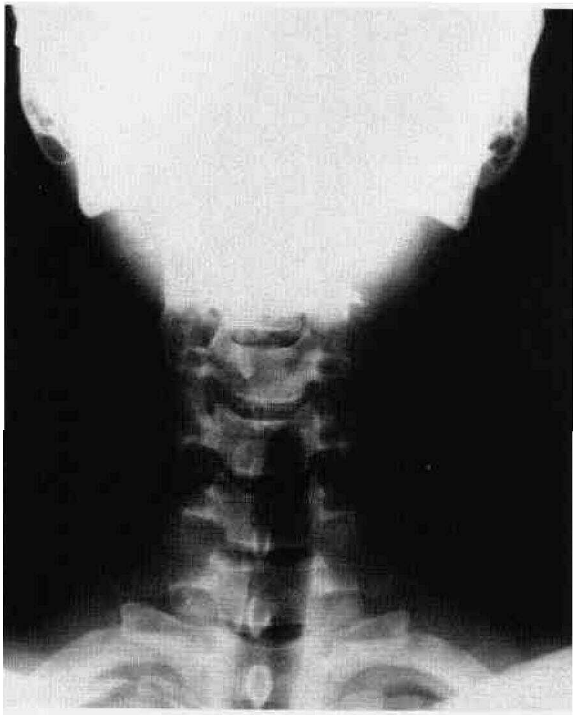

Figure 6-20 Normal AP projection cervical spine.

tified by plain radiography, and they require specialized imaging techniques, such as myelography, CT scan, and MRI, for appropriate evaluation and planning of treatment.[24]

In the region of the CV junction, skeletal lesions such as rheumatoid pannus, os odontoideum, odontoid fracture, platybasia, basilar impression, achondroplasia, and Paget's disease, which may have an impact on CNS function, can be rapidly and reliably identified by lateral and open mouth radiographs.[25] More specialized imaging techniques may not be indicated.

In the cervical, thoracic, and lumbar regions, plain radiographs may effectively identify degenerative and destructive lesions of the spine and demonstrate the effect of these lesions on the structural integrity of the spinal column; however, plain radiographs do not illustrate the impact of such lesions on the nervous system. Consequently, specialized imaging techniques are often employed prior to surgical intervention.

In the evaluation of vertebral trauma, plain radiography is normally the initial imaging technique. Lateral views are usually the most revealing, especially in the cervical and lumbar areas, and coupled with an AP view, these images pinay provide sufficient information to determine the need for stabilization or surgical intervention, particularly in the event of neurological deficits. A complete spine series may be required in symptomatic cases prior to concluding a normal examination or negative evaluation. In the event of positive physical or neurological findings and a negative plain radiographic examination, more specialized studies are often necessary. Table 6-1 details the suggested views for a complete series for each region of the spine.

COMPUTER ASSISTED IMAGING OF THE SPINE

Magnetic resonance imaging is the study of choice for the evaluation of abnormalities of the spinal canal, spinal cord, vertebral body marrow spaces, and intervertebral disk disease.[26] This is due to the absence of mobile protons in the cortical bone of the vertebral bodies and the neural arches, as well as the excellent soft tissue discrimination of MRI. MRI outlines the spinal cord within the CSF, allowing the differentiation of intramedullary and extramedullary lesions. It provides for the noninvasive diagnosis of primary spinal cord tumors (Fig. 6-22), syringohydromyelia, spinal cord demyelination or infarcts, and congenital malformations of the spinal cord or the spinal column. MRI is also ideal for the evaluation of pediatric spinal anomalies, i.e., meningoceles, myelomeningoceles, lipomyelomeningoceles, diaste-

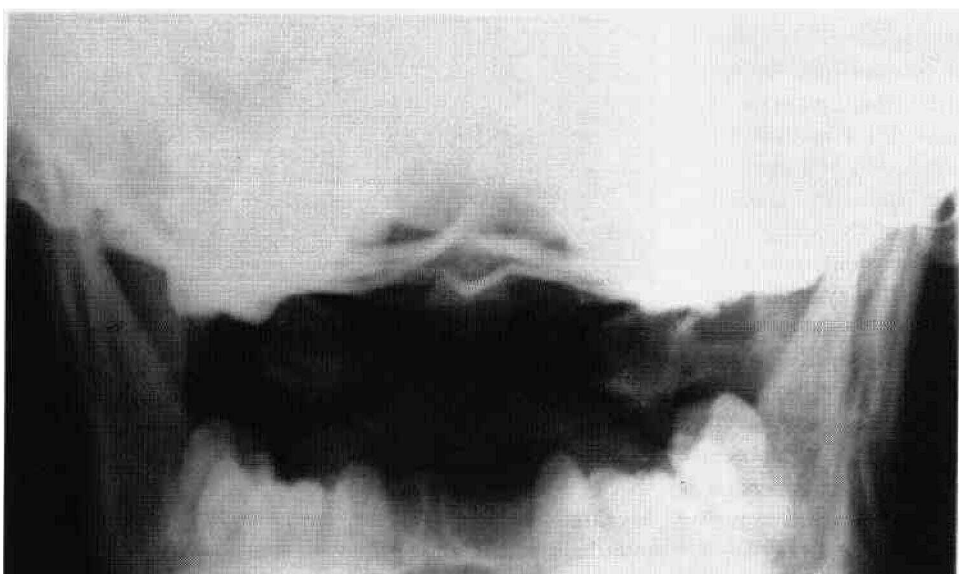

Figure 6-21 Open mouth view of odontoid. Note the symmetry of space between right and left lateral masses of CT and the odontoid process.

Table 6-1
SUGGESTED PLAIN RADIOGRAPHS IN THE EVALUATION OF SUSPECTED VERTEBRAL INJURY

Cervical Spine
1. Lateral
2. Anteroposterior
3. 30° Obliques
4. Upright weight bearing lateral
5. Flexion and extension laterals
6. Open mouth odontoid view of atlas and axis
7. Swimmers view of cervical thoracic junction

Thoracic Spine
M. Lateral
2. Anteroposterior

Lumbar Spine and Sacrum
1. Lateral
2. Anteroposterior lumbosacral spine
3. Anteroposterior pelvis

matomyelia, or tethered cord (Fig. 6-23). MRI with gadolinium-DTPA is recommended for investigation of neoplasms, both primary and metastatic, of the spinal canal.[27] Additionally, in patients with failed back syndrome, it can differentiate scar tissue from recurrent disk herniations (Fig. 6-24).

Limitations of MRI include the significant artifacts surrounding metallic hardware (Harrington rods, Halifax clamps, or metallic plates). Signal loss is also seen in areas of spinal surgery where metal deposition from use of surgical drills occurs, as in anterior cervical diskectomies. For this reason we routinely use diamond bits, but burrs are becoming available that do not leave behind materials that cause artifacts.

The use of MRI for evaluation of spinal lesions has changed the role of CT in recent years. At the present time, CT is the study of choice for evaluation of spinal trauma, especially when considering the presence of fractures or dislocations of the facets and/or neural arches. It is highly desirable to obtain a CT of the lower cervical spine to rule out lesions at the cervical-dorsal junction where plain radiographs of this region are of limited quality. CT is also used in evaluating burst fractures with retropulsion of fragments into the spinal canal, trauma to the spine by gunshot wounds, and abnormalities in alignment of the spine after deceleration injuries. Two- and three-dimensional reformatted CT images may also be helpful in the evaluation of complex injuries, developmental abnormalities, and degenerative changes of the spine (Fig. 6-25). There has been a continuous decline in the use of CT for the evaluation of routine lumbar spine diskogenic disease in favor of MRI. In cases where the MRI findings are equivocal, myelography in combination with CT (CT-myelogram) is recommended. The role of myelography and CT-myelogram is still important in the evaluation of abnormalities of alignment of the spine, including scoliosis and spondylolisthesis.

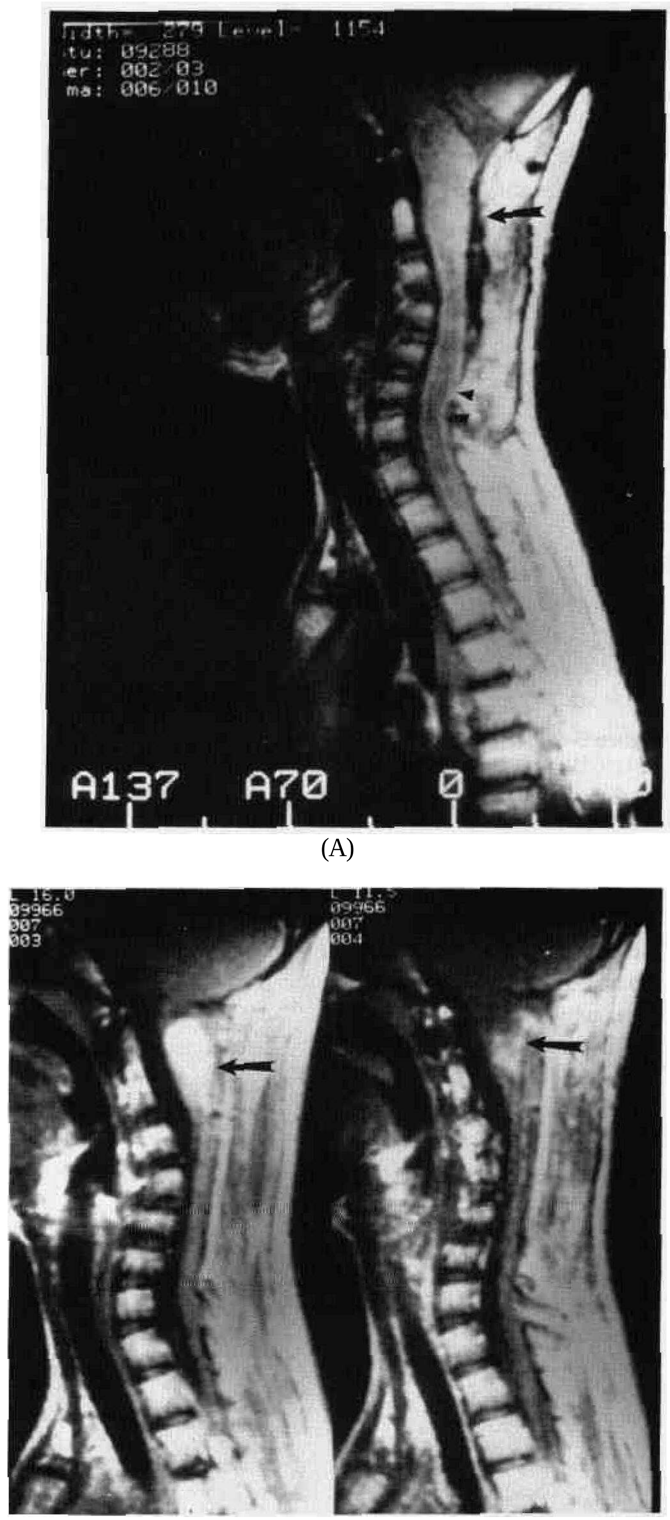

(A)

(B)(C)

Figure 6-22 Sagittal Tl image *(A);* sagittal T2 image *(B),* sagittal Tl image after administration of Gd *(C).*

MYELOGRAPHY

Myelography combines the use of contrast media injected into the subarachnoid space with spinal radiographs or polytomograms to outline the spinal cord and nerve roots. Walter

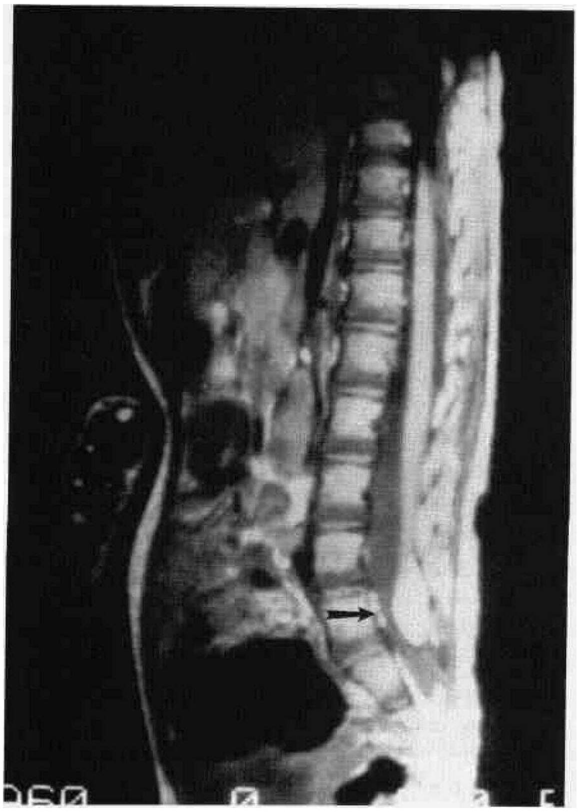

(A)

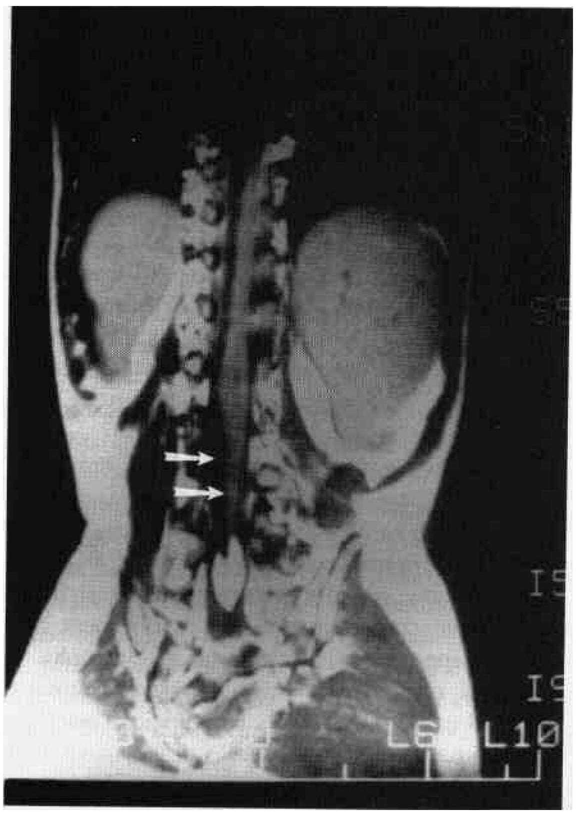

(B)

Figure 6-23 MRI of lumbar spinal region demonstrating lipoma with cord tethering. Sagittal Tl *(A).* Coronal Tl *(B).*

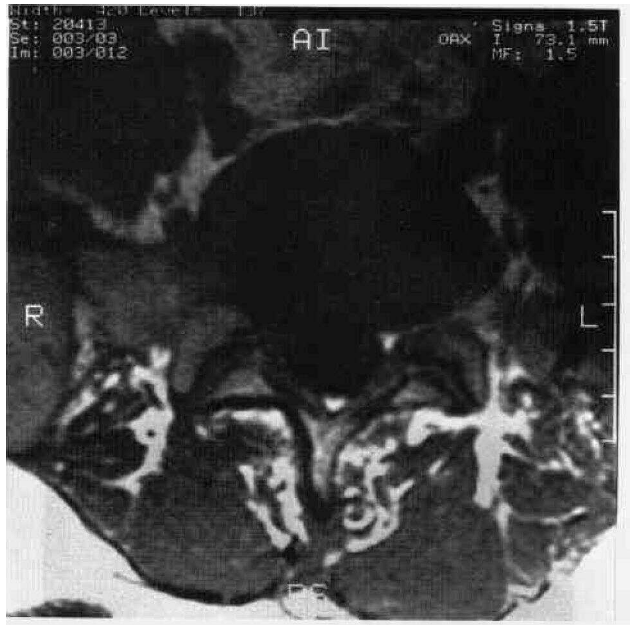

(A)

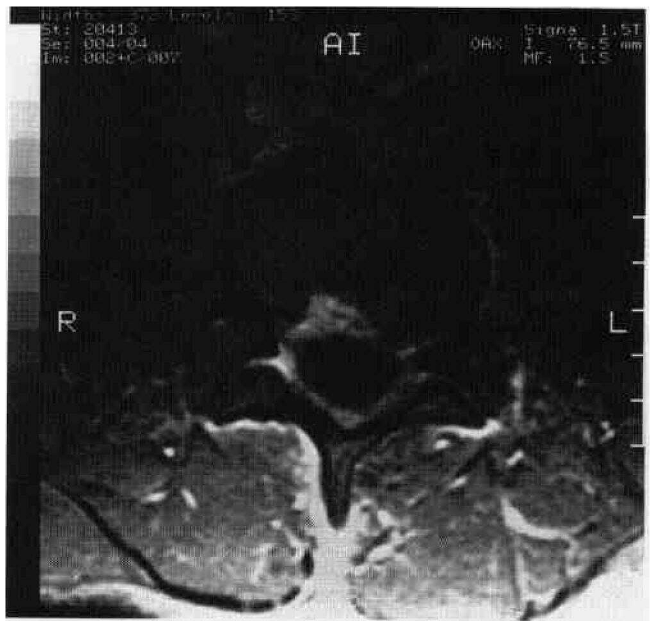

(B)

Figure 6-24 MRI of postsurgical lumbar spine *(A).* Axial Tl image with poor definition of dura/scar interface *(B).* Axial Tl image after Gd demonstrating dura/scar interface.

Dandy, in his 1919 paper on pneumoencephalography, advocated the use of air to contrast the subarachnoid space of the spinal column.[28] By 1921, Jacobeus in Sweden and Forestier and Sicard in Paris, using air and lipiodol, respectively, described the use of subarachnoid contrast media in the diagnosis of spinal cord tumors.[29] During the early 1940s, a less-viscous and less-toxic contrast medium was introduced, and myelography gained widespread use. With the availability of water-soluble contrast media by the mid-1970s came the capability for full volume opacification of the subarach-

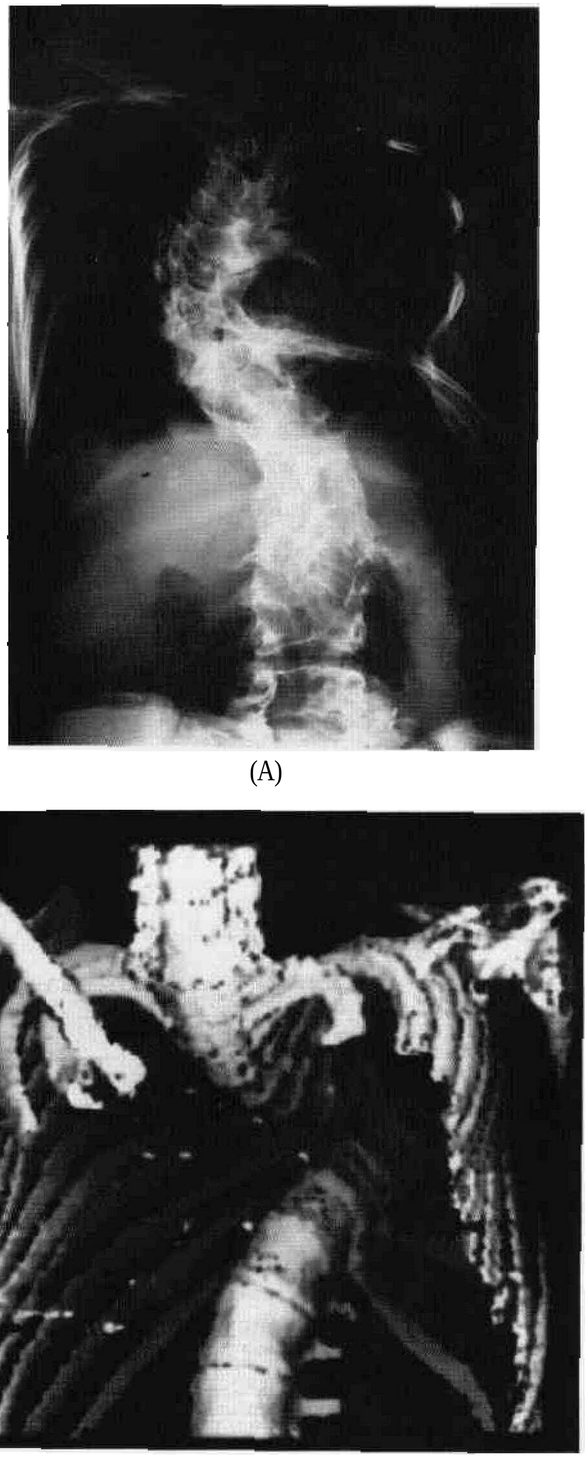

(A)

(B)

Figure 6-25 Scoliosis of thoracic and upper lumbar spine. *(A)* AP projection plain spine film. CT 3-dimensional reconstruction *(B).*

noid space, thus enhancing the diagnostic sensitivity and accuracy of myelography.[30]

The tandem combination of myelography and the post-myelogram CT were the mainstay in neuroradiology of the spine by the mid-1980s.[31] This combination affords multiple orientations from which to view the spinal canal and its contents. Myelography affords the versatility to focus on a specific region of the spine or a survey of the entire spinal axis. The patient may be repositioned during the study to simulate symptomatic postures or to facilitate the flow of contrast. Nerve root lesions and traumatic nerve root avulsions are often best demonstrated by myelography. Obstruction of the subarachnoid space (myelographic block) and cavitary spinal cord lesions, such as syringomyelia, may also be indicated by myelography; however, in general, the post-myelogram CT scan is more sensitive and more specific in the demonstration of spinal cord and spinal column lesions and may also identify lesions beyond the level of a complete myelographic block.

While a detailed discussion of the technique of myelography is beyond the scope of this text, some familiarity with the procedure will provide the insight necessary for selecting the appropriate imaging techniques.

The patient is placed on a radiolucent myelography table in the prone or a lateral decubitus (fetal) position in order to achieve separation of the spinous processes to provide easy access to the spinal canal. Mild sedation is frequently required; however, an awake, cooperative patient is preferred, and general anesthesia is seldom indicated.

The lumbar puncture is usually attempted at the L2-L3 level unless this is the area of particular interest. Adequate studies of the cervical, thoracic, and lumbar regions may be obtained via a lumbar injection of contrast provided meticulous attention to technique is maintained. Occasionally a cervical (C1-2) puncture and injection are necessary to obtain adequate opacification in the cervical region or to image the spinal canal above the level of a myelographic block. Once the needle enters the subarachnoid space and there is prompt return of CSF, the patient is positioned prone and the contrast medium is allowed to drip into the subarachnoid space. This aspect of the procedure should be observed under fluoroscopy to avoid a subdural or epidural injection. After the radiopaque contrast has been manipulated into the appropriate region, a series of lateral, anteroposterior, and oblique films is obtained. The protocol varies slightly between institutions. Depending on the diffusion of the contrast media and the extent of the study, a postmyelogram CT scan may be performed immediately or within 4 hours after the myelogram.

The indications for myelography are fairly broad—in essence, whenever there is a need to image the spinal cord or nerve roots. The most common application is in the evaluation of patients with neck pain, low back pain, and radicular pain; however, any complex of symptoms or signs which implicates spinal cord or nerve root involvement may be considered an appropriate indication for myelography. There are few, if any, contraindications to the use of water-soluble contrast myelography; however, neurological deterioration of patients with inflammatory diseases of the spinal cord has been reported after the use of some water-soluble contrast agents. In many institutions, myelography has been supplanted by MRI as the initial study of choice in the evaluation of the spine, particularly in an emergency.

In the normal myelogram, the radiopaque column that

Figure 6-26 Lateral projection of cervical myelogram. Note the dark shadow of the spinal cord outlined by the radiopaque water-soluble contrast. There is a slight disk bulge at the C5-6 level encroaching on the anterior meningeal space.

Figure 6-27 AP projection of cervical myelogram. The dark shadow of the spinal cord is centrally located within the canal and the nerve roots are demonstrated coursing inferolaterally from the spinal cord to the neural foramina.

results from water-soluble contrast media filling the subarachnoid space will exhibit regional variations due to the changes in the size of the vertebral canal, the size and trajectory of exiting nerve roots, and the cross-sectional diameter of the spinal cord. Nevertheless, there should be a uniform and symmetrical outline of the centrally positioned spinal cord from the upper cervical region to the level of the conus.

In the cervical region, the lateral projection usually demonstrates a relatively wide subarachnoid space ventral to the spinal cord and a narrower subarachnoid space posteriorly (Fig. 6-26). This is, in part, due to the moderate degree of extension in which the patient is positioned for cervical myelography. The anteroposterior diameter of the spinal cord viewed from the lateral projection remains rather uniform throughout the cervical region (Fig. 6-27). The anteroposterior projections should demonstrate uniform radiopaque margins bordering a central radiolucent shadow of the spinal cord, which may exhibit a slight increase in the cross-sectional diameter in the middle and lower cervical region. The fine linear radiolucencies of nerve rootlets are commonly outlined by the contrast within the subarachnoid space as they pass from the spinal cord and exit the neural foramina. Their appearance should be symmetrical at each segment. One common exception is presented by the occasional demonstration of perineural cysts, which fill with subarachnoid contrast material and give the nerve root sheath a bulbous appearance (Fig. 6-28). Usually, these cysts are not pathological.

In the thoracic region, the lateral projection outlines a spinal cord that adheres closely to the normal thoracic kyphotic curvature and demonstrates a constant anteroposterior diameter throughout the region (Fig. 6-29). The ventral subarachnoid space is usually denned by a fine radiopaque line separating the posterior aspect of the vertebral bodies from the radiolucent shadow of the spinal cord. The posterior subarachnoid space is much wider and remains uniform in its contour throughout the region. In the anteroposterior projections, the cross-sectional diameter of the spinal cord remains constant throughout the region; however, the subarachnoid space is narrowest in the midthoracic region and widens in the upper and lower thoracic regions (Fig. 6-30). The linear radiolucencies of the thoracic nerve rootlets, although not prominent, should be symmetrical. Thoracic myelography is frequently supplemented with polytomography or CT scan in a region of primary interest. A swimmer's view may be obtained if the cervicothoracic junction is suspect.

In the lumbar region, the subarachnoid space is usually

Figure 6-28 Oblique view cervical myelogram demonstrating perineural cysts of lower cervical roots.

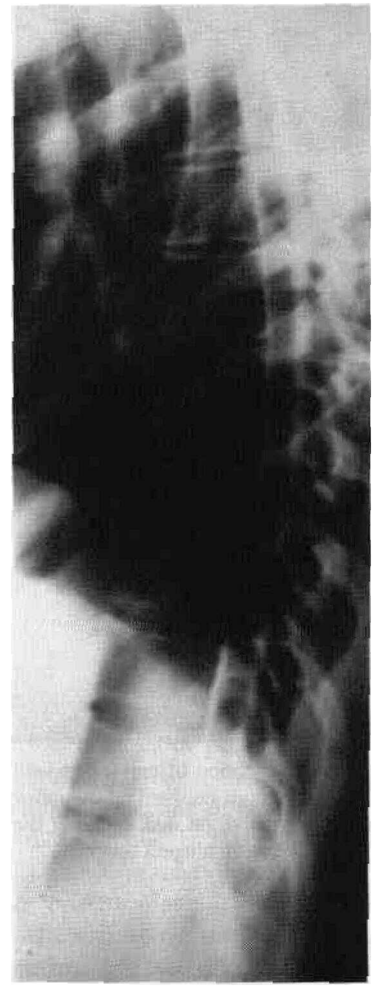

Figure 6-29 Lateral projection thoracic myelogram.

uniform in both the AP and lateral projections, down to the level of the lumbosacral junction. The caudal extent of the subarachnoid space may exhibit considerable variability but most often occurs below the S1 spinal level. The radiolucent shadow of the terminal segment of the spinal cord, the conus medullaris, should taper to a blunted point not lower than the L2 spinal level. In the lateral projection the collected radiolucencies of the cauda equina are usually observed in the posterior third of the lumbar subarachnoid space, with the fine linear radiolucencies of individual nerve roots coursing ventrally and caudally. In the AP projections, the paired nerve roots course caudally and laterally, ultimately turning lateral as they enter the neural foramina (Figs. 6-31 and 6-32). Occasionally, two nerve roots will share a common sheath as they exit ihe thecal sac *(conjoined nerve roots)*, thus giving an asymmetrical appearance. This is a normal anatomical variant.

The myelographic appearance of lesions involving the spinal cord may be placed into one of three categories: (1) extradural, (2) intradural extramedullary, and (3) intramedullary—each with a distinct myelographic pattern. Extradural lesions tend to displace the dura and the spinal cord to the opposite side, thus resulting in narrowing of the subarachnoid space between the lesion and the spinal cord and of the subarachnoid space between the spinal cord and the opposite side of the spinal canal. Depending on the size and orientation of the lesion and the projections being viewed, the contrast should outline a gentle curve around the lesion. Intradural-extramedullary lesions tend to displace the spinal cord and dura in opposite directions, thus widening the subarachnoid spaces, above and below and ipsilateral to the lesion. The contrast will outline the lesion, demonstrating a meniscus at its rostral and caudal poles. A myelographic block may result in the ability to visualize only one pole of the lesion. Intradural lesions in the lumbosacral region fill the subarachnoid space before they cause significant symptoms or signs. If they have not resulted in a complete myelographic block, the subarachnoid contrast will usually outline menisci at the rostral and caudal poles. Intramedullary lesions enlarge the radiolucent shadow of the spinal cord, thus narrowing the subarachnoid space on both sides of the cord. In most instances, lesions must be viewed from at least two projections in order to make the above distinctions, and some lesions may provide appearances not distinctive of one particular category. In these instances, a postmyelographic CT scan may be helpful.

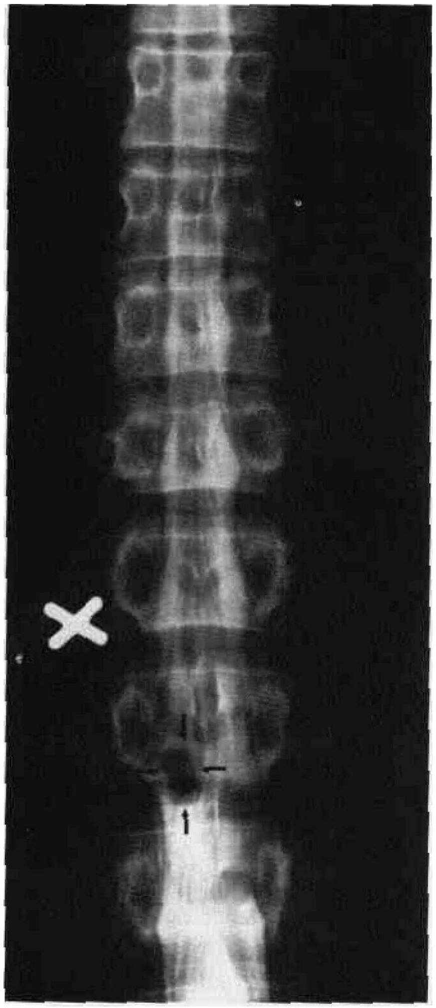

Figure 6-30 AP projection of lower thoracic and apper lumbar region. Note the symmetrical tapering of the conus at L.1-L2 and the intradural-extramedullary lesion *(arrows).*

Figure 6-31 Lateral projection lumbar myelogram.

Lesions that affect the filling of nerve root sheaths, producing filling defects, are usually described in the cervical and lumbosacral regions. The majority of these lesions are extradural defects resulting from herniations of intervertebral disks and degenerative diseases of the spinal column. The typical myelographic findings include defects of the ventral subarachnoid space on lateral projections and root sleeve effacements or filling defects at the same spinal level on the AP and oblique projections.

DISKOGRAPHY

Diskography involves the injection of small quantities of water-soluble contrast media into the nucleus palposis.[32] The placement of the needle and the injection of contrast media are performed with the aid of fluoroscopy, and subsequently plain radiographs of the region of interest are obtained. More than one disk space may be contrasted during the same study. The normal spinal disk will accept between 0.25 cc and 0.5 cc (cervical vs. lumbar, respectively) of contrast media, and they will distribute the contrast media in a smooth centrally positioned ellipsoid pattern. Injection of contrast material into a degenerated disk typically outlines a flattened disk space with an irregular contour. Tears in the annulus or fissures in the cartilaginous end plates may allow seepage of contrast to define a plane of separation between the degenerated disk and the adjacent vertebral bodies or the anterior and posterior longitudinal ligaments and over adjacent vertebrae (Fig. 6-33). During the injection, the patient's symptoms may be reproduced or exacerbated, thus suggesting a symptomatic degenerative disk.[33]

Diskography was popularized in the mid-1940s as a means of assessing the integrity of cervical and lumbar spinal disks. The information provided by this technique is limited to the intervertebral disk space and surrounding ligaments. Although an abnormal diskogram may be associated with reproduction of pain or other symptoms, many still question the validity of the technique in establishing a true cause-and-effeet relationship. The general acceptance and usefulness of this imaging technique in contemporary neuroradiology has declined since, under usual circumstances, MRI or myelography and CT scan provide sufficient information for clinical assessment and treatment planning. Diskography may be employed when there is need for intraoperative identification of the disk space or when the MRI

Figure 6-32 Oblique projection lumbar myelogram demonstrating multiple intradural mass lesions *(arrows).* Note the well-outlined nerve roots exiting the thecal sac and coursing obliquely toward the neural foramina.

Figure 6-33 Diskogram. Injection pattern of degenerated L4-L5 disk.

and myelogram and CT are equivocal and there is a need to reproduce symptoms.

ULTRASOUND IN NEUROLOGICAL SURGERY

Ultrasound uses sonic energy to produce images. Since the early 1970s, there have been dramatic improvements in ultrasonic imaging with a concomitant increase in utilization throughout medicine. This section reviews the physical principles and practical applications of ultrasound in neurosurgery.

PHYSICAL PRINCIPLES OF DIAGNOSTIC ULTRASOUND AND DOPPLER TECHNOLOGY

Ultrasonic imaging utilizes wave energy with frequencies higher than are audible to the human ear, i.e., greater than 20 kilohertz (kHz).[34] The probe, or transducer, emits and receives sound waves (Fig. 6-34). It contains piezoelectric (pressure-electric) crystals capable of converting sonic energy into electrical energy and vice versa. Each crystal is composed of charged molecules, i.e., dipoles. With a short

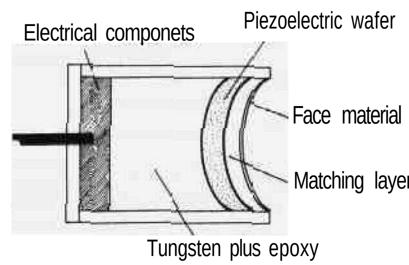

Figure 6-34 Ultrasound probe. Voltage is applied to the piezoelectric crystal, which produces a sound beam. The echoes reflected back at each tissue interface are converted to electrical impulses by the crystal and then displayed on a screen. Backing material dampens any energy directed opposite the patient and improves the image.

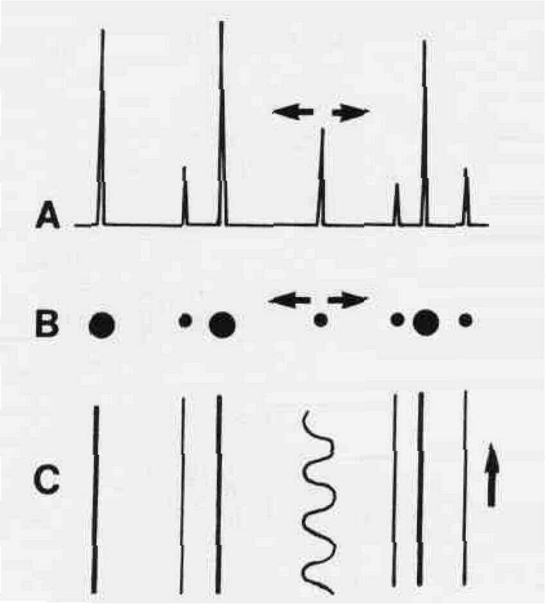

Figure 6-35 *A.* A Mode: Echoes are displayed as a function of distance from the probe. *B.* B Mode: The amplitude of the echo is proportional to the brightness of each dot. The dots are oriented in the same direction as the transducer. A 2-dimensional image is formed *(C).*

electrical pulse, the dipoles change their alignment and produce a sonic beam.[35-36] As the sonic beam is projected through tissue, some waves are reflected at each interface. The reflected waves (i.e., "echoes") are converted back into electrical impulses by the crystals and displayed.[36-37] In |diagnostic ultrasound, a short pulse of energy is transmitted, [followed by a longer listening phase when the transducer "receives returning echoes. Backing material, behind the crystal, dampens any energy directed opposite the patient, thereby reducing artifacts.[36]

The quality of the ultrasonic image is dependent on the frequency of the beam. With increasing frequency, the beam wavelength decreases, resulting in a short pulse length and better axial resolution. Higher-frequency beams have less tissue penetration. Focused transducers can collimate beams at a greater distance to help compensate for this. Lower-frequency transducers are better suited to examine deep lesions but at the cost of resolution.[35-38]

Modes of display of ultrasonic signals include A, B, and M modes, the B scan, and real time (Fig. 6-35). A mode (amplification) is one of the earliest and simplest forms of display. The image is displayed as a series of spikes. The stronger the echo, the larger the electrical signal and the higher the spike. Amplitude is represented on the *y* axis and depth on the *x* axis. Depth is calculated by the device using the velocity of sound at 1540 meters per second. A-mode imaging was used to identify midline structures in the head (echoencephalography), but it has rarely been used since the development of CT and MRI.[35-38]

Like the A mode, the static B, or brightness mode, represents only the current line of sight of the transducer. Each echo is displayed as a dot. The brightness of each dot is proportional to the intensity of the echo. B-mode scans generate static 2-dimensional images.[35-38] The TM (time-motion, or M motion) mode is used primarily in echocardiology, where the image displays the movements of various parts of the heart.[36]

Real-time ultrasound utilizes a rapid, sequential generation of 2-dimensional B-scan images. The images change almost instantaneously on the screen with shifts in the position of the transducer. The higher the rate of generation of images, the more fluid, or "real," the images appear. Most ultrasonic devices have a freeze-frame capability as well as memory, which allows the sonographer to outline normal and abnormal anatomy.[36,38] Real-time ultrasound may be used in conjunction with a Doppler to diagnose carotid stenosis.[34,38]

PHYSICAL PRINCIPLES OF DOPPLER TECHNIQUES

Whereas B-mode ultrasonic techniques are useful for deriving anatomical information, Doppler techniques provide physiological information on blood flow. The Doppler relates change in frequency of sound waves due to motion.[40] An example is the change in pitch of a warning siren from a police car as it moves toward and, subsequently, away from a stationary observer.[38]

To investigate blood flow velocity using a Doppler probe, an ultrasonic wave is directed toward the blood vessel. The wave front encounters moving blood cells, which cause a scattering of the transmitted sound such that the frequency shift is proportional to the velocity of the blood cells. The frequency of the returning sound waves is analyzed.[34,40]

A Doppler will detect returning echoes, calculate the shift, and display it audibly or visually as a frequency spectrum.[40] The echo from a normal blood vessel shows a spectrum of velocities representing laminar flow. In laminar flow the blood cells located more centrally move more rapidly than those in the periphery. An atherosclerotic plaque in the vessel causes turbulence or disruption in the normal laminar flow, and it may produce an increase in velocity at the site of stenosis. This may result in a broad range of frequency shifts known as *spectral broadening.*[3]*

There are two types of Doppler instruments: continuous" wave and range-gated. The continuous wave Doppler requires two crystal elements in the probe, one for transmission of sound waves and one for detection of the echoes. There is no depth resolution, and the Doppler will sample all structures within the range of the beam so that multiple vascular structures lying within the sample area may be indistinguishable.[34-40-41]

The range-gated Doppler uses short pulses of sound en-f ergy. The probe is gated to receive signals on the basis of depth. The echo is analyzed and a visual spectrum produced that evaluates individual vessels. However, only a small area may be analyzed at any one time. The range-gated Doppler is used to evaluate velocity or waveform patterns and turbulence within carotid arteries.[40,41]

The color flow Doppler employs a range-gated system that uses colors to depict velocity. It gives potentially faster and easier studies by rapidly identifying areas of high velocity or turbulence and allowing more-detailed Doppler studies of the abnormal areas. One color (usually red) indicates blood flowing in one direction and a second color (blue) indicates blood flowing in the opposite direction.[38] The technique is useful in evaluating the direction of flowing segments of an arteriovenous malformation during surgery.[42] Duplex sonography combines the anatomical information gained from real-time B scanners with physiological information obtained by the Doppler system.[43] The real-time ultrasound is used to determine the degree and severity of a stenosis and to localize the area analyzed by the Doppler. The computer in the duplex system performs spectral analysis and blood flow velocity calculations. Both the anatomy of the blood vessel and the velocity of blood flow can be determined simultaneously, potentially allowing calculation of flow volume.[40] Duplex sonography is used to screen for vascular stenosis.[43] Some institutions now prefer carotid endarterectomy based on duplex since it has a 90 to 95 percent sensitivity and specificity for carotid stenosis of greater than 50 percent.

CLINICAL APPLICATIONS OF ULTRASOUND AND DOPPLER TECHNOLOGY CEREBROVASCULAR IMAGING

Direct noninvasive evaluations of the carotid, vertebral, and subclavian arteries is accomplished with duplex sonography.[44,45] Duplex sonography combines anatomic information gained by real-time ultrasonography with physiological information gained by Doppler sonography.[43,44] It is inexpensive, noninvasive, easily reproducible, and places no stress on the patient.[44] Although the quality of real-time sonography decreases as the severity of the stenosis increases, the Doppler portion of the duplex scanner can be used to accurately identify rate-limiting stenosis.[38-45,46-47] As a screening procedure, duplex sonography is 97 percent sensitive.[48] A disadvantage of the method is its inability to identify stenosis of intracranial vessels.

In duplex sonography, the patient's neck is slightly extended and rotated to the side opposite the artery being examined. The transducer is used to scan the carotid artery from clavicle to mandible. Sonographic samples are taken from both common carotid arteries, external and internal carotid arteries, proximal vertebral arteries, and subclavian arteries. Hard copies of the analyzed data are retained for future reference (Fig. 6-36).[40]

Atheromatous plaques vary in type and size. They are commonly identified by real-time ultrasound. Small flat fibrofatty plaques are hypoechoic. Ulcerated plaques can contain surface variability, representing fibrous thrombi attached to the vessel endothelium. Ultrasound may be more accurate than arteriograms in identifying these ulcerated plaques.[49-50] Intraplaque hemorrhage is seen as a heterogenous pattern of low and medium echoes. Calcified plaques are recognized echogenic lesions that produce acoustic shadows.[47-51]

Real-time ultrasonography is used to determine areas for Doppler evaluation. Doppler analysis estimates velocity of blood flow. Velocity of blood flow is largely dependent on cardiac output, blood pressure, and the degree of stenosis.[40] With less that 50 percent stenosis, Doppler evaluation is not reliable. With stenosis of greater than 50 percent, there is an increase in peak systolic velocity, as well as spectral broadening. Between 75 percent and 90 percent stenosis, both the systolic and diastolic velocities are increased. With stenosis greater than 90 percent, the velocity decreases to normal and then subnormal values but displays a distorted waveform and a harsh sound. Low velocities are encountered in patients with poor cardiac output.[34-40] Spectral broadening throughout systole and diastole is indicative of more severe stenosis.[52] Doppler analysis uses peak systolic velocity, presence of spectral broadening, and the ratio of the velocities of internal to common carotid arteries to determine the degree of stenosis.[40]

There are limitations to duplex sonography.[34-40-43-47] The external carotid artery may be mistaken for the internal carotid artery when the internal carotid artery is occluded. The external carotid usually has a triphasic waveform indicative of high resistance, but it may take on a low-resistance pattern (Fig. 6-37). Also, severe stenosis may be falsely diagnosed as total occlusion if real-time ultrasound is unable to image the thin flow of red blood cells and Doppler sampling is not extensive enough to obtain a Doppler trace or supply through a collateral such as the ophthalmic artery. A color flow Doppler recording may facilitate the diagnosis.[38] Very severe stenosis may result in a normal flow velocity signal. Reduction in the diameter of the vessel of greater than 95 percent results in the return of flow to normal and then subnormal values. Care must be taken to analyze the waveform that is abnormal.[34-40-43-47]

Duplex sonography can also be used to evaluate stenosis at the origin of the subclavian arteries and to diagnose subclavian steal.[40] It is useful in the postoperative evaluation of flow in the external carotid to internal carotid bypass procedures and in assessing the patency of the carotid after endarterectomy.[38]

INTRAOPERATIVE CRANIAL SONOGRAPHY

Real-time ultrasonography is used to localize and characterize intracranial lesions during surgery. Tumors, abscesses, cysts, and arteriovenous malformations have acoustic properties that differ from normal brain tissues. Intraoperative sonography is useful in outlining subcortical or deep-brain lesions; it often indicates the best route of dissection to the lesion and ultimately decreases surgical time and morbidity. When using ultrasound in the operating room, it is desirable to have a technician handle the details. It may be necessary to have an ultrasonologist to interpret the images if the surgeon is not experienced.[53-56]

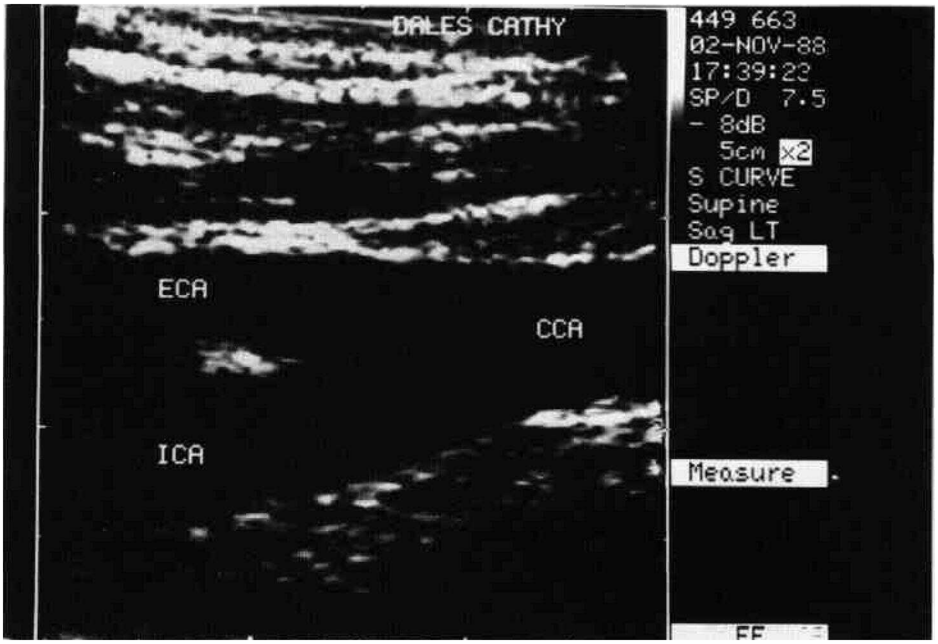

(A)

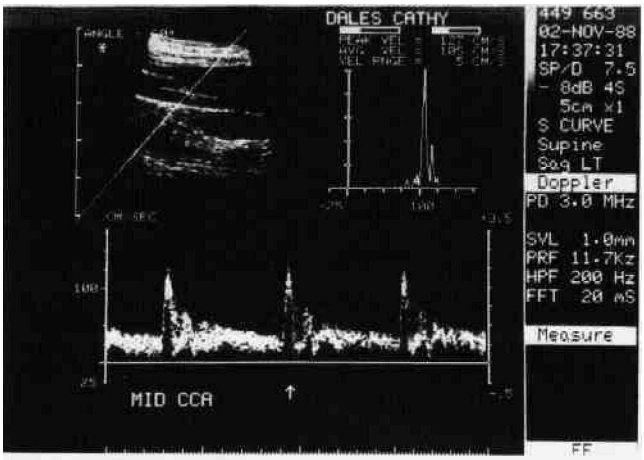

(B)

Figure 6-36 *A.* Sagittal image of a normal carotid bifurcation. *B.* Real-time image of a normal carotid bifurcation in top left corner with sample volumes (=) taken in the CCA. The real-time fast Fourier transform analysis (FIT) shows a normal waveform profile for the CCA.

By employing an instrument guide attached to the probe, a biopsy needle or cannula is directed to a specific point. In this way, tumors can be biopsied and cystic lesions appropriately drained.[54-57∧62] If areas within a tumor differ in echogenicity, samples may be obtained from different areas; this allows for more accurate pathological identification. When draining cysts or abscesses, ultrasonic guidance is essential. A probing cannula may fail to penetrate an abscess. Adjustments may be required to penetrate the lesion. Ultrasound, therefore, will relate the probe to a tumor or cyst and indicate appropriate corrections during the course of a procedure. The site of a lesion is monitored after removal of the cannula to rule out postbiopsy hemorrhage.[54,57,59,62,64]

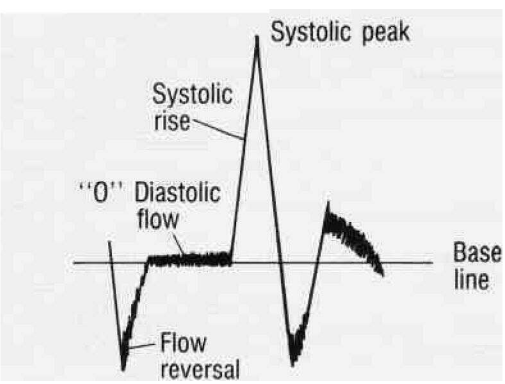

Figure 6-37 Example of triphasic waveform of the external carotid artery.

Although the specific pathology of tumors cannot be identified by sonography, tumors generally have a greater echogenicity than brain and appear hyperechoic.[54-64] Metastatic lesions are often subcortical and have well-defined borders.[54-64-65] Ultrasound differentiates the cystic from the solid portions of tumors.[53-63,66] Low-grade gliomas are hyperechogenic on ultrasound and may have well-defined borders, whereas high-grade gliomas have poorly defined borders.[54-64] Areas of necrosis within tumors can be identified as more echogenic than true cysts, which appear black

Figure 6-38 Longitudinal intraoperative sonogram of spinal cord tumor. Cyst can be visualized within the spinal cord.

on sonography.[53] Calcification within tumors causes acoustic shadowing. Areas of edema surrounding tumors can be differentiated on ultrasound from actual infiltration by the tumor.[59,63-64] Feeding vessels or major cerebral vessels located near tumors can be identified.[57] By ultrasonic imaging, intracerebral abscesses have a well-defined hyperechoic rim with a hypoechoic center. Septations within an abscess cavity can be visualized.[55,58-64]

Arteriovenous malformations are echogenic, and most can be localized by standard gray scale real-time ultrasonography.[56] More useful is the color-flow Doppler sonography of vascular malformations. This produces an image in which the color red is encoded for flow in one direction and the color blue for flow in the opposite direction. Thus, a malformation and its feeding arteries and draining veins can be quickly and easily located. Prior to closure gf the craniotomy, the area can be scanned to detect any residual malformation or complicating hematoma. Intraoperative sonography can also be used to locate small mycotic aneurysms and to help determine the patency of cerebral vessels after placement of aneurysm clips.[42]

Intraoperative sonography is used to locate missiles, bone, and other debris embedded within the cerebrum after trauma. It has been found helpful in the placement of ventricular catheters for shunts or Ommaya reservoirs, especially in patients who have very small ventricles. Imaging is performed through open fontanelles in infants and through small trephines in adults. Malposition of ventricular catheters can be accurately determined and immediately corrected.[54,58-59,62-63-67]

INTRAOPERATIVE SPINAL SONOGRAPHY

Ultrasonography has been utilized in the management of a variety of spinal lesions, including resection of intramedullary and extramedullary tumors, placement of shunts into syringes, decompression of traumatic fractures, location of herniated disks, and in the management of congenital anomalies such as Chiari malformations.[68-74]

Intraoperative sonography can be performed with the pa-

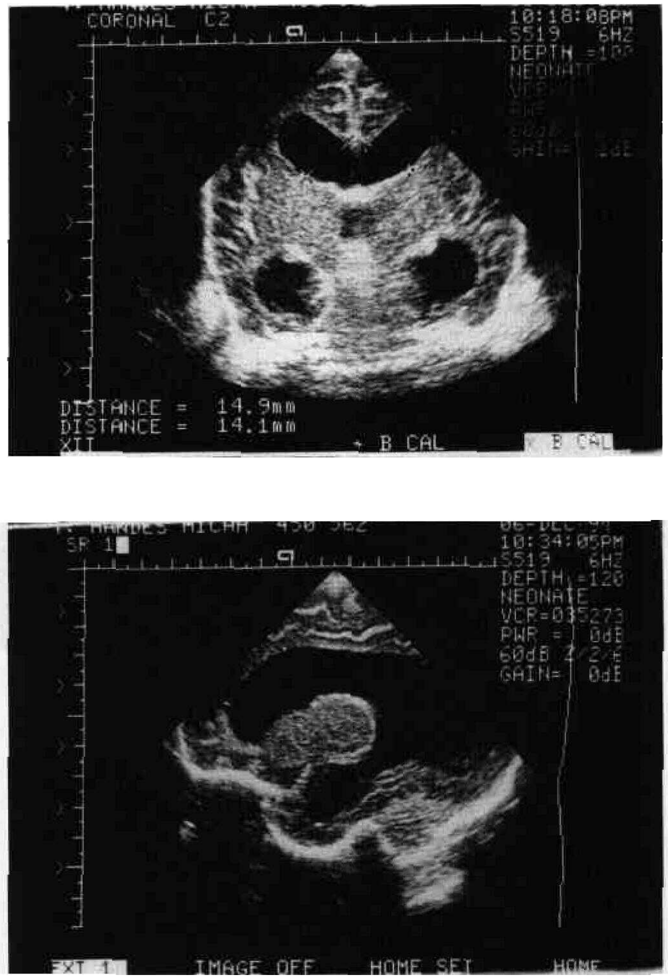

(B)

Figure 6-39 Coronal sonogram through dilated lateral ventricles and third ventricle with large temporal horns *(A).* Parasagittal sonogram shows dilatation of one lateral ventricle, trigone, and temporal horns *(B).* No atrophy of parenchyma is seen.

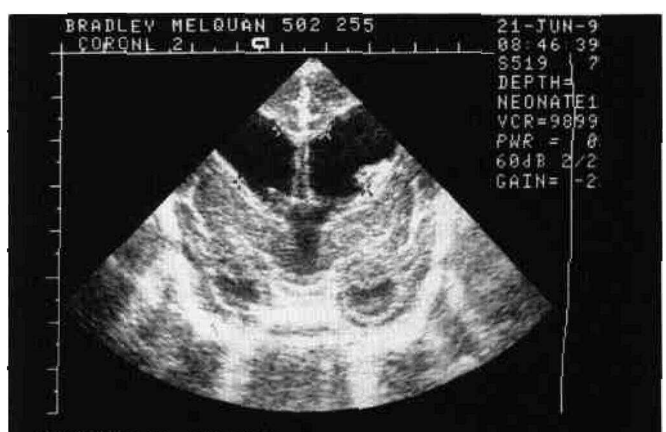

Figure 6-40 Grade III intraventricular hemorrhage. Note hyperechoic areas that represent hemorrhage in the lateral ventricle. Ventricles are markedly dilated.

nent in the supine or prone position but not in the lateral position. After the laminectomy is performed, the wound is tilled with sterile saline to prevent near-field artifact and to ivoid direct contact of the probe with the spinal cord and serve roots. Usually a 7.5 MHz transducer is used for •isualization, although it may be desirable to use 10 MHz. The spinal cord, nerve roots, dentate ligaments, intervertebral disks, and vertebral bodies can be imaged without opening the dura. The area is examined systematically in the transverse and sagittal planes. An initial examination is performed to establish the landmarks and to locate lesions. Sonography can then be performed during the course of surgery to monitor progress and, at the termination of the case, to document the extent of resection or decompression.[68,72-75]

Intraoperative sonography can identify tumors and delineate the margins for biopsy or resection. Intramedullary tumors are typically isoechoic or hyperechoic when compared to the normal spinal cord. Cystic and solid portions of a tumor may be clearly identified (Fig. 6-38). Sonography shows expansion of the cord and concomitant narrowing of the subarachnoid space. The normal central echo of the cord is absent and is thought to represent the transition zone from normal cord into tumor.[70-73,75-76]

Sonography can differentiate intramedullary from extramedullary masses. Extramedullary masses—i.e., meningiomas, neurofibromas and lipomas—are usually homogeneous and hyperechoic as compared to normal spinal cord. They have well-defined borders. Sonography reveals compression of the spinal cord and enlarged subarachnoid spaces above and below the lesions.[68,71-73-75]

Extradural lesions such as metastases or herniated disks are imaged as hyperechogenic masses which narrow the subarachnoid space. If large, the mass may compress the spinal cord and obliterate the central echo in the cofd. Stretching of nerve roots can also be imaged. Scar tissue, however, can mimic disk protrusion or metastases.[68-73,75]

Intraoperative sonography is useful in monitoring the degree of reduction of a fracture without manipulating the spinal cord.[69-77,78] A laminotomy no larger than 1 square centimeter will permit introduction of an ultrasonic probe to visualize the area.

Intraoperative sonography can be used to localize bone and missile fragments within the canal and is particularly useful when these fragments are mobile. The image generally conforms to the shape of the fragment. Sonography can also detect syringomyelia, myelomalacia, pseudomeningocele, dural tears, tethered cord, and arachnoiditis.54,69,73,75

A syrinx within the spinal cord is imaged as an anechoic space with well-defined borders. It is typically surrounded by abnormal spinal cord. The size and number of cystic cavities and the presence of septations are all easily demonstrated. Sonography can direct placement of the catheter into the syrinx and monitor the amount of reduction. If decompression is inadequate, immediate surgical maneuvers, such as catheter manipulation, can be performed.[63,70,73-75]

Intraoperative sonography can be used to image the posterior fossa after bony decompression of a Chiari malformation. If sonography shows that the decompression is inadequate, a patch graft and plugging of the obex can be performed when the surgical management involves decompression of the fourth ventricle and dissection of the vermian peg from the medulla7i-«,79,8o,8i

TRANSCRANIAL DOPPLER SONOGRAPHY

Transcranial doppler (TCD) sonography was introduced in 1982 by Aaslid.[82] It is a noninvasive, easily reproducible technique for determining blood flow velocities in the major intracranial arteries. A special transducer is used to insonate the basal cerebral arteries directly through the squamous portion of the temporal bone, the orbit, and the foramen magnum. The most common application of TCD sonography has been in the evaluation of cerebral vasospasm. TCD sonography can also be used intraoperatively to monitor cerebral blood flow.[83] The physical principles of TCD sonography are essentially the same as Doppler sonography of carotids except that a lower frequency is used.

The internal carotid, anterior cerebral, anterior communicating, posterior cerebral, and posterior communicating arteries are insonated through the squamous portion of the temporal bone. The carotid and ophthalmic arteries, carotid siphon, and, occasionally, the anterior cerebral artery are insonated through the orbit. A low-power setting must be used to reduce the ultrasonic exposure to the eye. Through the suboccipital approach, the vertebral and basilar artery signals are obtained.[82-83]

Descriptions of the methods for localizing each of the basal arteries can be found in detail elsewhere.[84] Normal values of the velocities for the various cerebral vessels are available for comparison.

In contrast to arteriography, TCD sonography is noninvasive, easily reproducible, and can be performed at the bedside. It has been used clinically in the evaluation of cerebral vasospasm.[35-85,86] It is a sensitive measure of the development as well as resolution of vasospasm. Flow velocity is inversely related to vessel diameter. With vasospasm, the vessel diameter decreases, and TCD sonography records the increased velocity in the artery. This is used as a guide for treatment of the patient.

TCD sonography is used intraoperatively to identify pathological flow patterns during carotid endarterectomy or open heart surgery. EEG or other electrophysiologic monitoring is indirect and often shows changes only after tissue injury has occurred. TCD sonography detects a disruption of flow before any ischemic injury has developed.[34-83] TCD sonography has also been used intraoperatively to localize AVMs and their feeder vessels.[87] The utility of TCD sonography is being assessed in the evaluation of increased intracranial pressure, in monitoring cerebral flow in seizure patients, in the evaluation of ventriculomegaly and hydrocephalus, and in intraoperative monitoring for cerebral emboli, as well as confirmation of brain death.[83]

EXAMINATION OF THE NEONATE WITH ULTRASOUND

Ultrasonography is used to screen neonates for intraventricular hemorrhage, congenital malformations, and tumors (Fig. 6-39). Testing is often performed in the nursery, minimi/ing stress to the infant. Since the examination is noninvasive and involves no radiation, scans can be repeated frequently. For most infants, a 5- or 7.5-MHz probe is used to insonate through the anterior or posterior fontanelle for visualization of the intracranial structures.[88,89]

Premature infants are screened for intraventricular hemorrhage within the first 3 days of life (Fig. 6-40). Ultrasonography has a sensitivity of 96 percent and specificity of 94 percent for diagnosing intraventricular hemorrhage.[84] If indicated, follow-up scans can be easily obtained. Over a period of weeks, the hematoma changes to a hypoechoic area surrounded by an echogenic rim. With time, the area develops into a porencephalic cyst which appears anechoic.[38,89-91]

Ultrasonography of the craniocervical junction via the posterior cervical approach provides good visualization of the medulla, tonsils, vermis, and cervical cord in infants because the posterior arches of the cervical spine are minimally ossified. This allows evaluation of the infants for a Chiari malformation and for evidence of intracranial hemorrhage.[92-93] Other congenital malformations that can be evaluated by Ultrasonography include the Dandy-Walker syndrome, agenesis of the corpus callosum, holoprosencephaly. lissencephaly, and schizencephaly, among others.[91-93]

In summary, tumors have a greater echogenicity than normal brain. Ultrasound is also used to evaluate tumors in infants. Cysts, necrosis, and calcifications can be identified, but the specific pathology cannot be determined by ultrasound alone. It may also be difficult to differentiate infarctions or hemorrhage from tumor. CT scan or MRI scan is required for further evaluation.[38]

SUGGESTED READING

Ramsey RG: *Neuroradiology*. 2d ed. Philadelphia, Saunders, 1987.
Burrows EH, Leeds NE: *Neuroradiology*. New York, Churchill Livingstone, 1981.
Kirkwood JR: *Essentials of Neuroimaging*. New York, Churchill Livingstone, 1990.
Daffner RH: *Imaging of Vertebral Trauma*. Rockville, Md, Aspen, 1988.
Gehweiler JA Jr, Osborne RL Jr, Becker RF: *The Radiology of Vertebral Trauma*. Philadelphia, Saunders, 1980.
Petersen HO, Kieffer: Neuroradiology, in Baker AB, Baker LH (eds): *Clinical Neurology*. Philadelphia, Harper & Row, 1987.

REFERENCES

1. Pendergast EP, Schaeffer JP, Modes PJ: *The Head and Neck in Roentgen Diagnosis*, 2d ed. Springfield, 111, Charles C. Thomas, 1956.
2. Hoursfield N: A method of and apparatus for examination of a body part by radiation such as x-ray or gamma radiation. British Patent 1283915, 1972.
3. Ambrose J: Computerized transverse axial scanning (tomography): II. Clinical application. *Br J Radiol* 41:1023-1047, 1973.
4. Villafana T: Physics and instrumentation, in Lee SH, Rao KCVG (eds): *Cranial Computed Tomography*. New York, McGraw-Hill, 1985, chap 1, pp 1^6.
5. Williams AL: Trauma, in Williams AI, Haughton VM (eds): *Cranial Computed Tomography*. St. Louis, Mosby, 1985, pp 37-87.
6. Smith FW: NMR—Historical aspects, in Newton TH, Potts DG (eds): *Modem Neuroradiology*, vol 2: *Advanced Imaging Techniques*. San Francisco, Clavadel Press, 1983, pp 7-14.
7. Bradley WG, Crooks LE, Newton TH: Physical principles of NMR, in Newton TH, Potts DG (eds): *Modem Neuroradiology*, vol 2: *Advanced Imaging Techniques*. San Francisco, Clavadel Press, 1983, pp 15-61.
8. Bradley WG: Effect of magnetic relaxation times on magnetic resonance image interpretation. *Noninvasive Med Imaging* 1:195-204, 1984.
9. Wehrli FW, MacFall Jr, Newton TH: Parameters determining the appearance of NMR images, in Newton TH, Potts DG (eds): *Modern Neuroradiology*, vol 2: *Advanced Imaging Techniques*. San Francisco, Clavadel Press, 1983, pp 81-117.
10. Weinman HJ, Gries H, Speck U: Gd-DTPA and low osmolar Gd chelates, in Runge V (ed): *Enhanced Magnetic Resonance Imaging*. St. Louis, Mosby, 1989, pp 74-86.
11. New PFJ, Rosen BR, Brady TJ, et al: Potential hazards and artifacts of ferromagnetic and nonferromagnetic surgical and

STUDY QUESTIONS

I. A 28-year-old male was involved in an automobile accident in which he was thrown from the car. He sustained multiple abrasions of the head and body but no gross deformities. Over the next 2 days he become progressively more alert but complained of neck pain.

1. What imaging and/or radiographic study(ies) might be recommended upon admission to the emergency room? Why? 2. Which imaging study might be most likely to show evidence of subarachnoid hemorrhage within the first 24 hours? 3. What imaging study might best demonstrate evidence of cerebral contusion after 6 days? Why? 4. What imaging study might best demonstrate evidence of a fractured odontoid process? 5. What imaging study would most likely show evidence of a basilar skull fracture?

II. A 60-year-old male who had known carcinoma of the prostate began complaining of midthoracic back pain and gradually developed weakness, first in his left lower extremity, then the right. A plain x-ray of the thoracic and lumbar spine showed multiple areas of increased density and other areas of erosion.

1. What initial imaging study might best demonstrate the extent of bony involvement with metastases? 2. What imaging study might best demonstrate a specific site of involvement of the spinal canal which could account for the paresis? 3. What is the classic study that would have been used to demonstrate evidence of a spinal block? 4. What would be the expected appearance of a partial spinal block by myclography? 5. What imaging study would most likely demonstrate evidence of a fracture? *

III. A 60-year-old diabetic hypertensive Caucasian lady is admitted with a sudden onset of left hemiparesis and right monocular blindness, each of which lasted for a half-hour. Both cleared. The patient had a bruit over the right carotid artery.

1. What scanning study should be used to indicate evidence of disease of the carotid artery? 2. What study would most likely demonstrate evidence of cerebral damage initially? 48 hours later? 3. What would Dopplcr flow studies of the carotid artery show if the carotid artery were 60 percent occluded? 80 percent occluded? 4. Under what conditions might a direct arteriogram be required? 5. What might an MRI of the head show?

IV. An infant was born at 30 weeks of gestation. Within the day he developed a full fontanel and persistent drowsiness.

1. What diagnostic evaluations might be considered? 2. Assuming an intracerebral hemorrhage, what forms of imaging might be used to follow the progress of the hemorrhage? 3. What form of imaging might be used to follow the progress of hydrocephalus? 4. What imaging study might demonstrate the sight of aqueductal stenosis? 5. How might a subependymal hemorrhage be differentiated from a subarachnoid hemorrhage on CT?

V. A 25-year-old male suddenly complained of the "worst headache I've ever had in my life" and then lost consciousness. He was also nauseated, vomited twice, and had a stiff neck.

1. What imaging study would most likely indicate the cause of the headache? 2. Assuming evidence of subarachnoid hemorrhage, how might the source be first identified? 3. How might an aneurysm be identified noninvasively? 4. What is the best imaging examination to outline discretely the aneurysm? 5. How might one determine evidence of chronic vasospasm noninvasively?